

Republic of Iraq  
Ministry of Higher Education and Scientific Research  
University of Babylon / College of Science  
Department of Physics



**Study The Nuclear Properties for Even-Even  $^{224-234}\text{Th}$   
Isotopes by Using The (IBM-1)**

A Thesis

Submitted to the council of College of Science University of Babylon as a  
partial fulfillment of the requirements for the Master degree in Physics  
Science

**By**

**Nibras Haider Hammoud Attia**

B.Sc. in Physics (2018)

**Supervised by**

**Prof.Dr.**

**Mohsin Kadhim MuttalebAl-Janaby**

**Lect.Dr.**

**Ghaidaa A. Hafedh Jaber**

**2023 A.D.**

**1445 A.H.**

بِسْمِ الْعَظِيمِ

﴿ إِنَّ فِي خَلْقِ السَّمَاوَاتِ وَالْأَرْضِ وَاخْتِلَافِ اللَّيْلِ  
وَالنَّهَارِ لآيَاتٍ لِّأُولِي الْأَبْصَارِ ﴾

صَدَقَ اللهُ الْعَلِيِّ الْعَظِيمِ

(سورة آل عمران/آية ١٩٠)

### Supervisors Certification

We certify that this thesis entitled (**Study The Nuclear Properties for Even-Even <sup>224-234</sup>Th Isotopes by Using The (IBM-1)**) was prepared by (**Nibras Haider Hammoud Attia**) under our supervision at Department of Physics, College of Science, University of Babylon, as a partial fulfillment of the requirements for the practical work of Master degree in Physics Science.

**Signature :**

**Supervisor:**

Dr.Mohsin Kadhim MuttalebAl-Janaby

**Signature :**

**Supervisor:**

Dr. Ghaidaa A. Hafedh Jaber

**Title :** Professor

**Address:** Department of Physics

College of Science-

00

**Title :** Lecture

**Address:** Department of Physics

College of Science-

**Date :**     /     /2023

### Certication of the Head of the Department

In view of the available recommendation, I forward this thesis for debate by the examination committee.

**Signature:**

**Name:** Dr. Samira Adnan Mahdi

**Title:** Assistant Professor

**Address:** Head of the Department of Physics ,College of Science, University of Babylon

**Date:**     /     / 2023

## *Dedication*

*To all the beams of my life, mother... to the everlasting symbol of prosperity, my father ,my sisters ,my family... my close friend ... whom I met and I was pleased that I did, my friends and colleagues.*

*Nibras*

## *Acknowledgments*

*First of all, I should thank my Almighty (Allah) for helping me in completing my Thesis.*

*I would like to express my thanks and gratitude to my supervisors **Prof. Dr. Mohsin Kadhim Muttaleb Al-Jnaby** and **Lec. Dr. Ghaidaa A. Jaber Hussien** for suggesting this topic for me and for their distinguished efforts and sound advice and directions that helped me. In alleviating all the difficulties, I encountered during my work,*

*Many thanks are due to the college of sciences at the University of Babylon and the Department of Physics for offering me the opportunity to complete my Thesis.*

*My great thanks to my friends for their kind help and support.*

*Many thanks and gratefulness to my family who always support me and alleviate difficulties I have faced during my works.*

*Nibras*

## Summary

The Interacting Bosons Model-1 (IBM-1) was used to find the optimal Hamiltonian for energy level calculations and the reduced probability for a quadrupole electric transition  $B(E2)$  for the nuclei of various even-even isotopes.

The energy levels,  $B(E2)$  and electric quadrupole moment  $Q$  of the levels were calculated for the number of transitions of the even-even isotopes ( $^{224}\text{Th}$ ,  $^{226}\text{Th}$ ,  $^{228}\text{Th}$ ,  $^{230}\text{Th}$ ,  $^{232}\text{Th}$ ,  $^{234}\text{Th}$ ) using the best fitted coefficients in the Hamiltonian equation using the interacting bosons model-1 (IBM-1).

As well as identifying the shape of the nuclei by studying the surface potential energy using the equations of the potential energy function, which gives an idea of the nucleus deformation from contour line deviation and assembly in a specific region.

The results matched experimental data. Branching ratios ( $R$ ,  $R'$ , and  $R''$ ) were calculated. The location of the elements relative to the three determinations  $SU(3)$ ,  $O(6)$  and  $U(5)$  is important in determine the shape of the nucleus and the deformation that occur in it. The results showed that the isotopes  $^{224} - ^{234}\text{Th}$  are located in the  $O(6)$ - $SU(3)$  transition region .

## *Contents*

No.	Subject	Page No.
	Summary	I
	Contents	II
	List of Symbols	III
	List of Figures	VI
	List of Tables	VII
	<b><i>Chapter One: General Introduction</i></b>	<b>(1-17)</b>
1.1	Introduction	1
1.2	Nuclear Models	3
1.2.1	Liquid Drop Model	3
1.2.2	Shell Model	5
1.2.2.A	The Single Particle Shell Model	6
1.2.2.B	The Spin-Orbit Coupling Potential	8
1.2.3	Collective Model	9
1.3	Residual Interaction	10
1.4	Review of the literature	11
1.5	The Aim of the Research	17
	<b><i>Chapter Two Interacting Boson Model(IBM-1)</i></b>	<b>(18-34)</b>
2.1	Interacting boson model	18
2.2	IBM-1 Hamiltonian	19
2.3	Electric Transitions	21
2.4	Dynamical Symmetries	22
2.4.1	Vibrational Limit of The IBM-1 U(5)	23
2.4.2	Rotational Limit of The IBM-1 SU(3)	25
2.4.3	$\gamma$ -Unstable Limit of The IBM-1 O(6)	28
2.5	Transitions Regions in IBM-1	30

No.	Subject	Page No.
2.5.1	Type 1 : $U(5) \rightarrow O(6)$	32
2.5.2	Type 2 : $O(6) \rightarrow SU(3)$	32
2.5.3	Type 3 : $U(5) \rightarrow SU(3)$	32
2.5.4	Type 4 : $U(5) \rightarrow SU(3) \rightarrow O(6)$	33
2.6	Surface Potential Energy	33
<b><i>Chapter Three: Results and Discussion</i></b>		<b>(35-58)</b>
3.1	Introduction	35
3.2	Calculation Energy Levels	35
3.3	B(E2) reduced electric transition	42
3.4	B(E2)Branching Ratios	50
3.5	Surface Potential Energy	52
<b><i>Chapter Four: Conclusion and Future Works</i></b>		<b>(58-59)</b>
4.1	Conclusions	58
4.2	Future Works	59

### *List of Symbols*

Symbol	Definition
IBM	The interacting boson model.
IBFM	The interacting boson fermion model.
$U(6)$	The unitary group.
$U(5)$	Vibrational Limit.
$SU(3)$	Rotational Limit .
$O(6)$	$\gamma$ -Unstable limit .
$N_p$	Total number of neutron bosons or proton bosons.

$N$	The neutron number.
PES	Potential energy surface.
$\beta$	The deformation parameter.
$\gamma$	The angle of deviation from symmetry axes.
$\hat{H}$	The Hamiltonian operator in IBM-1.
$s^\dagger, d^\dagger$	The creation operators for $s$ and $d$ bosons.
$\tilde{s}, \tilde{d}$	The annihilation operators for $s$ and $d$ bosons.
$n_d$	The total number of d-boson.
$n_s$	The total number of s-boson.
eb	Electron barn
$\varepsilon$	The boson energy
$\varepsilon_s$	The energy of s- boson.
$\varepsilon_d$	The energy of d- boson.
$a_0$	The strength of the pairing interacting between the bosons.
$a_1$	The strength of the angular momentum interacting between the bosons.
$a_2$	The strength of the quadruple interacting between the bosons
$a_3$	The strength of the octupole interacting between the bosons
$a_4$	The strength of the hexadecapole interacting between the bosons
$\hat{P}$	The pairing operator.
$\hat{L}$	The angular momentum operator.
$\hat{Q}$	The quadruple operator.
$\chi$	The quadruple structure parameter.
$\hat{T}_3$	The octoupole operator.

$\hat{T}_4$	The hexadecapole operator.
$\hat{T}^{E_2}$	The electric quadrupole operator.
$\hat{T}^{M_1}$	The magnetic dipole operator.
$\hat{T}_m^{(E_2)}$	The general multiple E2 operator of the IBM-1
$E_2SD = \alpha_2(e_b)$	The effective charge of s-d boson.
$E_2DD = \beta_2$	The effective charge of d-d boson.
$ \langle I_i    \hat{T}^L    I_f \rangle ^2$	the matrix element of (E2) transition
B(M1)	Reduced magnetic dipole transition probability.
$\nu$	The number of d-boson not paired to zero angular momentum called seniority.
$n_\Delta$	The number of d-boson tripled coupled to zero angular momentum.
L,M	The two quantum numbers which represent the angular momentum and components.
$\lambda, \mu$	The two quantum numbers which represent the Casimir operator, represent cases SU(3).
K	The number of cases that have equal values of $(\lambda, \mu, L)$ .
$\sigma$	The number of d-boson not pairwise coupled .
$\tau$	The number of d-boson not pairwise coupled to zero angular momentum.
R, R', R''	The branching ratio.
$E(N, \beta, \gamma)$	The potential energy surface

### *List of Figures*

Figure No.	Subject	Page No.
1.1	picture of a nucleus as a drop of incompressible liquid	4
1.2	Radial dependence of different mean potentials: Square Well $V_{sq}$ , Harmonic Oscillator $V_{ho}$ , and <i>Woods-Saxon</i> Potential $V_{ws}(r)$ (drawn here for $R = 10a$ )	7
2.1	A typical spectrum and a quantum numbers for U(5) symmetry	25
2.2	A typical spectrum and a quantum numbers for SU(3) symmetry	28
2.3	A typical spectrum and a quantum numbers for O(6) symmetry	30
2.4	The Casten triangle	31
2.5	Ideal scheme for potential energy surface	34
3.1	The ratio $(E_{4_1^+}/E_{2_1^+})$ has been compared with experimental data	36
3.2	The ratio $(E_{6_1^+}/E_{2_1^+})$ has been compared with experimental data	37
3.3	The ratio $(E_{8_1^+}/E_{2_1^+})$ has been compared with experimental data	37
3.4	The arrangement of energy levels for $^{224}\text{Th}$ , theoretical and experimental	39
3.5	The arrangement of energy levels for $^{226}\text{Th}$ , theoretical and experimental	40

3.6	The arrangement of energy levels for $^{228}\text{Th}$ , theoretical and experimental	40
3.7	The arrangement of energy levels for $^{230}\text{Th}$ , theoretical and experimental	41
3.8	The arrangement of energy levels for $^{232}\text{Th}$ , theoretical and experimental	41
3.9	The arrangement of energy levels for $^{234}\text{Th}$ , theoretical and experimental	42
3.10	$B(E2; 2_1^+ \rightarrow 0_1^+)$ comparison for all isotopes	50
3.11	Symmetric shape and potential distribution for $^{224}\text{Th}$	53
3.12	Symmetric shape and potential distribution for $^{226}\text{Th}$	54
3.13	Symmetric shape and potential distribution for $^{228}\text{Th}$	55
3.14	Symmetric shape and potential distribution for $^{230}\text{Th}$	55
3.15	Symmetric shape and potential distribution for $^{232}\text{Th}$	56
3.16	Symmetric shape and potential distribution for $^{234}\text{Th}$	57

*List of Tables*

Table No.	Subject	Page No.
3.1	Energy ratios for each limit are typical	36
3.2	Values for Hamiltonian parameters as in IBM program	38
3.3	B(E2) experimental data and its coefficients (E2SD, E2DD)	43
3.4	Electric transitions B(E2) for $^{224}\text{Th}$	44

Table No.	Subject	Page No.
3.5	Electric transitions B(E2) for $^{226}\text{Th}$	45
3.6	Electric transitions B(E2) for $^{228}\text{Th}$	46
3.7	Electric transitions B(E2) for $^{230}\text{Th}$	47
3.8	Electric transitions B(E2) for $^{232}\text{Th}$	48
3.9	Electric transitions B(E2) for $^{234}\text{Th}$ .	49
3.10	Two electric transition branching ratios	51
3.11	The coefficients of potential energy as in IBM program	52

# *Chapter One*

## *General Introduction*

### **1.1 Introduction**

As a result of the complex nature of nuclear forces and the entry of many factors into it, the possibility of studying the nuclear structure in a detailed theoretical way has become very difficult, as many of the experimental results did not agree with the theoretical conclusions. For this reason, nuclear models were developed to describe the nuclear structure. The other influencing is to obtain the exact structure of the nuclei (fine structure) with some mathematical approximations. Several nuclear models have appeared, and among these models is the Liquid Drop Model, which was proposed by (Von Weisker and Nils, 1935) [1]. According to this model, the bonding between nucleons was envisioned similar to the bonding of liquid molecules. One of the hypotheses of this model is that the nucleus consists of incompressible matter, and the nuclear force is equal for all nucleons, and in particular it does not depend on being protons or neutrons. This model showed aggregate properties, but it failed to explain the stability of the nucleus and the nature of the nuclear forces that bind nucleons. As a result, the shell model appeared by (W. Elasser, 1974) [2].

This model found an explanation for the magic numbers and other nuclear properties in terms of the effect of the nucleus as a whole on the individual nucleons, and with this model we get energy levels consistent with the existence of magic numbers, and another characteristic that supports the shell model is its ability to find the total angular momentum in the case of even-even nuclei ,

since the protons and neutrons are in the form of pairs, and therefore the intrinsic angular momentum and the orbital momentum of these nuclei cancel each other out, and this result is consistent with the practical observations that the total angular momentum of the even-even nuclei in their ground state is equal to zero, while the odd-odd nuclei are equal to the number correct.

However, the shell model failed to explain a number of nuclear properties, the most important of which is that this model assumes the shape of the nucleus is spherical (the quadrupole moment is zero), but it has been proven practically that the heavy nuclei are not spherical in shape, as well as cases of high spin ( $i_{13/2}$ ,  $h_{11/2}$ ) predicted by this model did not appear in the practical results, as well as a failure with regard to zero transitions that are so important that exact knowledge of them gives an idea of the exact structure of the nucleus [3].

Following the failure of the shell model, another model appeared called the unified model (the total motion model), as whenever the number of nucleons deviates from the magic numbers, cooperative effects begin to appear between the nucleons, and that the basis of this model is dependence on the distortion that affects the nucleus due to the increase in nucleons and interaction in this model. Totally (collectively) between the nuclei, and this gives a fixed shape to the nucleus. It is assumed here that the nucleus rotates completely, as this rotation is small compared to the rotation of a single nucleus. [3, 4]. In (1976) put together a compilation model by (Arima and F. Iachello) [5, 6], and studied by (T. Otsuka). This model is called the Interacting Boson Model, as this model succeeded in studying the spectra of the lower energy levels of nuclei with medium and heavy mass numbers. This model does not differentiate between pairs of protons and neutrons and is called (IBM-1).

That the attempt to understand and explain the nuclear properties and the nature of interactions between nucleons and the practical results related to them led to the development of theories based on some important physical foundations to become the basic rule in theoretical calculations with the addition of several influential factors to suit the practical results that this complex problem of nuclear structure was addressed by these mathematical estimates Under the heading Nuclear models [7].

## **1.2 The Nuclear Models**

Among these models that studied the nuclear structure are:

### **1.2.1 Liquid drop model:**

This model was proposed by (Von Weizsacker, 1934), who explained the binding energy and the phenomenon of nuclear fission, but did not succeed in giving an explanation for the stability of the nucleus. The nuclear bond of a single nucleon takes a fixed value for most of the elements, and also that the nuclear substance does not depend on the type of substance, but rather it is a fixed value. those nuclear particles. This model was able to explain nuclear fission, as when the nucleus is exposed to an external particle (when it is bombarded with a neutron or the nucleus captures a neutron), the nucleus begins to vibrate (like a drop of liquid), and this continuous vibration leads to its fission into two nuclei, each smaller than the nucleus, but it is preserved. On the ratio of the number of protons and neutrons. This model was also used to estimate the radius of the nucleus. Perhaps the most important success of this model is its ability to calculate the mass of the nucleus through a semi-empirical relationship [8]

then the Figure (1.1) picture of a nucleus as a drop of incompressible liquid roughly accounts for the observed variation of binding energy of the nucleus.

According to liquid drop model, the mass of an atomic nucleus is given by [9]:

$$m \approx Zm_p + Nm_n - \frac{E_B}{c^2} \quad (1.1)$$

where ( $m_p$ ) and ( $m_n$ ) are the rest mass of a proton and a neutron, respectively, and ( $E_B$ ) is the binding energy of the nucleus. The semi-empirical mass formula states that the binding energy will take the following form [9]

$$E_B = a_V A - a_S A^{\frac{2}{3}} - a_C \frac{Z(Z-1)}{A^{\frac{1}{3}}} - a_A \frac{(A-2Z)^2}{A} + \delta(A, Z) \quad (1.2)$$

where  $a_V$  = volume term,  $a_S$  = Surface term,  $a_C$  = Coulomb term,  $a_A$  = Asymmetry term and  $\delta(A, Z)$  = Pairing term.

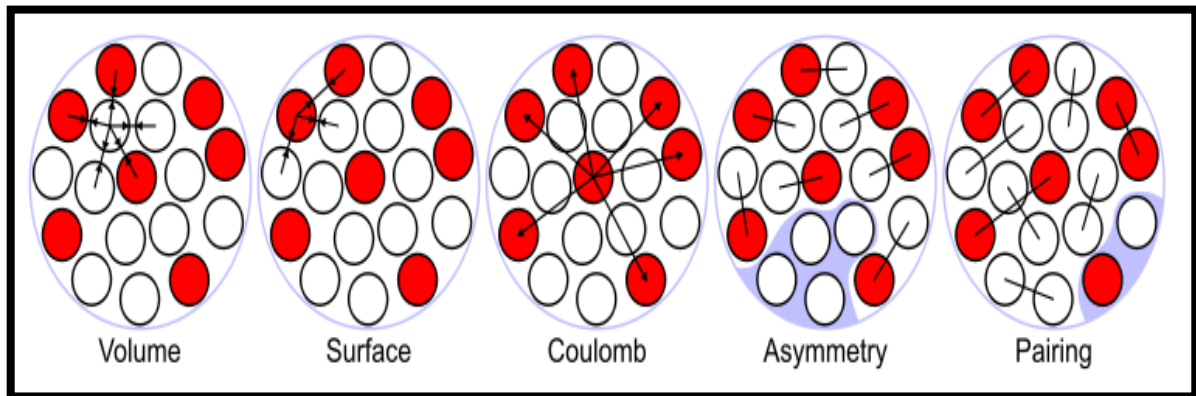


**Figure (1.1)** picture of a nucleus as a drop of incompressible liquid [10]

**Volume Energy:** When an assembly of nucleons of the same size is packed together into the smallest volume, each inside nucleon has a certain number of other nucleons in contact with it. So, this nuclear energy is proportional to the volume.

**Surface Energy:** A nucleon at the surface of a nucleus interacts with fewer other nucleons than one in the internal of the nucleus and hence its binding energy is less. This surface energy term takes that into account and is therefore negative and is proportional to the surface area.

**Coulomb Energy:** The electric repulsion between each pair of protons in a nucleus contributes toward decreasing its binding energy.

**Asymmetry Energy (also called Pauli Energy):** An energy associated with the Pauli exclusion principle. Where it not for the Coulomb energy, the most stable form of nuclear matter would have the same number of neutrons as protons, since unlike numbers of neutrons and protons imply filling higher energy levels for one type of particle, while leaving lower energy levels unoccupied for the other type.

**Pairing Energy:** An energy which is a correction term that arises from the tendency of proton pairs and neutron pairs to occur. An even number of particles is more stable than an odd number [10].

### 1.2.2 Shell model:

This model was proposed by W. Elsasier,1935) [11]. Practical experiments have shown that the stability of the nucleus is high when the number of nucleons is equal to one of the magic numbers (Magic Numbers) . In addition to that, he determined the angular momentum of the energy levels, but he failed to explain the nuclear spin of the ground level of the even-even nuclei, which is always equal to zero. It also did not address the effect that distorts the spherical shape of the nucleus caused by nucleons outside the closed shell [12].

The shell model succeeded in explaining the phenomenon of magic numbers in which the nucleus is highly stable, as well as determining the angular momentum of the energy levels of the nucleus, but this model was unable to find an explanation for the quadrupole moments of some nuclei that contain nucleons outside the closed shell[2].

### 1.2.2.A The Single Particle Shell Model

In the single particle shell model, the nucleons in the nucleus are assumed to move in common potential. The paired nucleons form an inert core of zero spin and zero magnetic moment. Consequently, the predicted spin and magnetic moment of even-even nuclei is zero. Odd-A nuclei properties are characterized by unpaired nucleon and for odd-odd nuclei by unpaired proton and neutron [13].

Shell closure properties electromagnetic and nuclear state properties are obtained in terms of the uncorrelated motion of single particles in the specified mean potential. The nuclear potential is expected to fall between two extremes: the infinite square well and the infinite harmonic oscillator potentials. This potential which has experimental basis is the Woods-Saxon potential. It is flat at the center and falls off smoothly to zero at the edge of the nucleus and is given by [11]:

$$V_{WS}(r) = \frac{-V_0}{1+e^{(r-R)/a}} \quad (1.3)$$

The parameters in this model of the potential have been evaluated to be approximately:

$$V_0 \approx 57 \text{ (MeV) + Corrections.} \quad R = 1.2A^{1/3} \text{ fermi, (A) is the mass number.}$$

$a = 0.65$  fermi.

where ( $V_0$ ) is the depth of the potential, ( $r$ ) is the distance from the center to the surface of nucleus, ( $a$ ) determines how clearly the potential increases to zero and ( $R$ ) is the radius at which  $V_{WS}(r) = -V_0/2$ . The other correction for protons is the electrostatic repulsion energy, which takes the form

$$V(r) = \begin{cases} \frac{ZKe^2}{R_c} \left[ 1 + \frac{1}{2} \left( \frac{r}{R} \right)^2 \right] & r < R_c \\ \frac{ZKe^2}{r} & r > R_c \end{cases} \quad (1.4)$$

where ( $R_c$ ) is the critical charge radius, distinct from  $R$ . The model radius for the nuclear potential, the approximate potentials for neutrons and protons, take the general form shown in Figure (1.2).

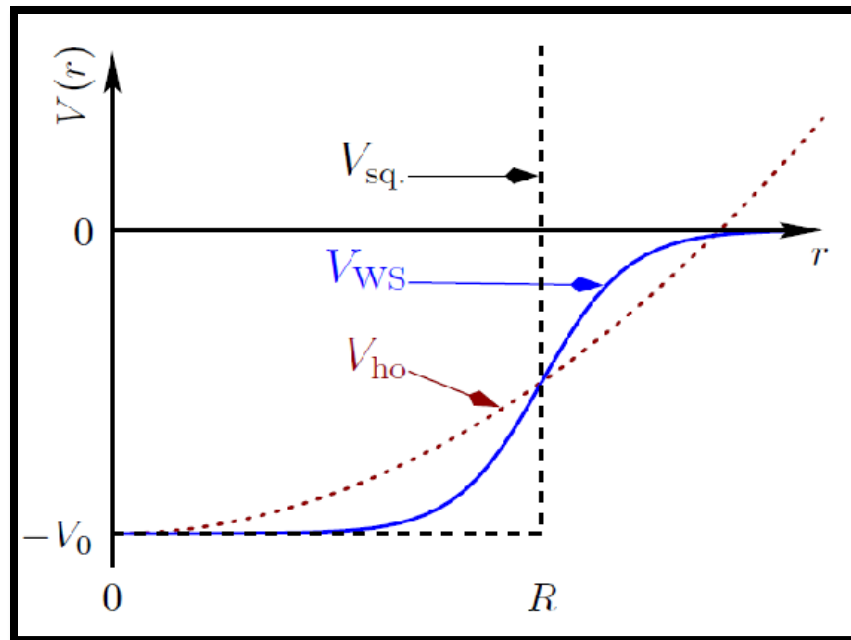


**Figure (1.2)** Radial dependence of different mean potentials: Square Well  $V_{sq.}$ , Harmonic Oscillator  $V_{ho}$ , and Woods-Saxon Potential  $V_{ws}(r)$  (drawn here for  $R = 10a$ ) [13]

An exact solution for the Woods-Saxon potential cannot be obtained, and numerical methods are employed.

### 1.2.2.B The Spin-Orbit Coupling Potential

The experimental observation of magic numbers and additional potential was done by Haxel, Jensen, and Suess [14] and independently by Otsuka, T. (2022) [15]. They recognized the missing ingredient in the shell model presented so. The added attractive interaction potential is usually written as:

$$V_{\ell,S} = -V_{\ell,S}(r) \vec{\ell} \cdot \vec{S} \quad (1.5)$$

where  $(\vec{S})$  and  $(\vec{\ell})$  are the spin and orbital vectors for the nucleon. They proposed that strong interactions should exist between the orbital angular momentum and the intrinsic spin angular momentum of each nucleon. They suggested that each energy level might be split into two levels. According to the quantum-mechanical coupling rules for angular momenta, the total angular momentum( $\vec{j}$ ) is formed by the vector addition of the orbital angular momentum( $\vec{l}$ ) and the intrinsic spin( $\vec{s}$ ). When nucleons have parallel orbital and spin angular momenta they occupy lower energy level. In the higher level, the orbital and spin angular momenta are antiparallel (that is,  $j = \ell \pm 1/2$ ). The coupling term can split the energy level of a state into two levels with coupling term having two nucleons

$$\langle \vec{\ell} \cdot \vec{S} \rangle = \frac{\hbar^2}{2} \begin{cases} \ell & \text{for } j = \ell + \frac{1}{2} \\ -(\ell + 1) & \text{for } j = \ell - \frac{1}{2} \end{cases} \quad (1.6)$$

If a strong spin-orbit interactions should exists, a different energy is associated with each of these two values of ( $j$ ), and gives rise to a spin-orbit splitting of the levels. Each state of the given ( $j$ ) may accommodate  $(2j+1)$  neutrons or protons. The shell closures occur at particles numbers (2, 8, 20, 28, 50, 82, and 126) exactly as seen by the experiments .

### 1.2.3 The collective model:

This model was proposed by (Boher & Mottelson, 1952), which led to the division of the nucleus into central nucleons and nucleons outside the center, as the center treats as a liquid drop that interacts with the outer nucleons in the unfilled shells [16].

The successes achieved by both the shell model and the liquid drop model can lead to real difficulties in front of the comprehensive nucleus theory, because each of them is contradictory to the other in terms of the basic hypotheses and premises on which it was based. As well as their interpretation of different nuclear properties of the same nuclei. Therefore, it is not possible to cancel the role of either of them. This in turn leads to the conclusion that the two models represent two incomplete parts of a broader and more comprehensive model that includes aspects of both the liquid drop model and the crust model, which is called the collective model [17].

After that, (Arima & Iachello) [5,6] proposed a new nuclear model to describe the nuclear composition of medium and heavy nuclei, except for magic nuclei or semi-magic nuclei [18,19], as nucleons were treated outside the closed shells the principal nuclei of the even-even pairs, as pairs of protons and neutrons, are called bosons, which have the ability to interact with each other

and have an intrinsic momentum equal to zero. [20,21] Through this model, (Arima & Iachello) was able to describe the characteristics of the energy levels in the nuclei. Even-even with medium and heavy mass numbers as pairs of nucleons outside the closed shell that were treated as bosons so that the degrees of freedom of these bosons were not taken into account.

It was called the first interacting boson model [22] IBM-1 This model, which was proposed by (Arima & Iachello) in the year (1974), is one of the nuclear models that succeeded in finding most of the nuclear properties, as it gives good theoretical values close to the practical values, especially with regard to energy levels and its ability to explain The decay of excited nuclear levels that lead to the emission of gamma rays as they decay.[23]

### 1.3 Residual Interaction

The models discussed above, emerging both particle and collective characteristic of the nucleus, have effectively exchange the particle interactions by a potential which is, generally, time dependent and non-spherical. this potential cannot take into consideration the whole interaction between particles and a weak interaction can yet be supposed to exist.

Utilizing techniques inserted in superconductivity theory, Belyaev studied the impact of a pairing force between the particles and found that the inclusion of this force could interpret the energy gap (i.e the absence of agitated states below  $\sim 1$  MeV) observed in even – even nuclei [24]. The calculations were expanded by Kisslinger and Sorenson (KS) who included, in addition to the pairing force, a long range quadrupole interaction. these two forces have little opposing effects, the pairing interaction tending to couple nucleons to zero

angular momentum producing a spherical shape while the quadrupole force tends to correlate the motion of the nucleons giving rise to collective characteristics (quadrupole vibrational) in the energy level spectrum. The resultant wave functions for the nuclear states are thus a linear combination of particle and particle plus phonon wave functions. These authors have calculated many nuclear properties for nuclei from nickel to lead, not including the strongly distorted region ( $150 < A < 190$ ). The agreement with experiment is, in many cases, very impressive. For example, in the even – even isotopes the agreement between theoretical and experimental reduced electric quadrupole transition probabilities, i.e., the  $B(E2)$  values, is commonly within a factor of two [25].

## 1.4 Review of the literature

We will review the literature study for some authors:

**In (2013)[26] A. I. Levon *et al*** , studied the excitation spectra in the deformed nucleus  $^{228}\text{Th}$  have been studied by means of the (p,t) reaction, using the Q3D spectrograph facility at the Munich Tandem accelerator. The angular distributions of tritons were measured for about 110 excitations seen in the triton spectra up to 2.5 MeV. Firm  $0^+$  assignments are made for 17 excited states by comparison of experimental angular distributions with the calculated ones using the chuck3 code. Moments of inertia have been derived from these sequences, whose values may be considered as evidence of the two-phonon nature of most  $0^+$  excitations. Experimental data are compared with interacting boson model and quasiparticle-phonon model calculations and with experimental data for  $^{229}\text{Pa}$ .

**In (2016) [27] A. Leviatan and D. Shapira** present a symmetry-based approach for prolate-oblate and spherical-prolate-oblate shape coexistence, in the framework of the interacting boson model of nuclei. The proposed Hamiltonian conserves the  $SU(3)$  and  $\overline{SU(3)}$  symmetry for the prolate and oblate ground bands and the  $U(5)$  symmetry for selected spherical states. Analytic expressions for quadrupole moments and E2 rates involving these states are derived and isomeric states are identified by means of selection rules.

**In (2016)[28] S. Sharma**, the interacting boson model Hamiltonian was used to describe the energy spectrum,  $B(E2)$  value and  $B(E2)$  branching ratios for inter-band and intra-band transitions for three quasi-bands in  $^{146}\text{Sm}$ . It is found that IBM-1 reproduces the observed complex nuclear structure very well. The agreement between the theoretical results and the observed data are satisfactory for all possible observed nuclear properties. Present results are compared with the dynamic pairing-plus-quadrupole model, IBM-2 and previous interacting boson approximation calculations.

**In (2017)[29] S. Y. Leea *et al***, studied the study of structure in  $^{224-234}\text{Th}$  nuclei within the framework IBM, An investigation has been made of the behavior of nuclear structure as a function of an increase in neutron number from  $^{224}\text{Th}$  to  $^{234}\text{Th}$ . Thorium of mass number 234 is a typical rotor nucleus that can be explained by the  $SU(3)$  limit of the interacting boson model(IBM) in the algebraic nuclear model. the low-lying energy levels and E2 transition ratios corresponding to the observable physical values are calculated by adding a perturbed term with the first-order Casimir operator of the  $U(5)$  limit to the  $SU(3)$  Hamiltonian in IBM. We compared the results with experimental data

of  $^{224-234}\text{Th}$ . Lastly, the potential of the Bohr Hamiltonian is represented by a harmonic oscillator, as a result of which the structure of  $^{224-234}\text{Th}$  could be expressed in closed form by an approximate separation of variables.

**In(2017)[30] N. Al-Dahan** , studied descriptive study of the even-even actinide nuclei  $^{230-234}\text{Th}$  isotopes using IBM-1 and it found the nuclear structure of the actinide even–even thorium isotopes from  $A=230-234$  have been investigated within the framework of the Interacting Boson Model (IBM-1). Predictions are given for the excited state energies for the ground state,  $\beta$  and  $\gamma$ -bands, the transition probabilities between these states, the rotational moment of inertia, and the energy staggering in the  $\gamma$ -band energies. The results of these calculations are compared with the experimental data on these isotopes.

**In(2018)[31] S. B. Doma and H.S. EI- Gendy** , studying a nuclear phenomenological study of the even–even thorium isotopes  $^{228-232}\text{Th}$ , and it found The rotational and vibrational energies and the electric transition probability  $B(E2)$  of the even–even  $^{228-232}\text{Th}$  isotopes are studied empirically in framework of a nuclear phenomenological approach by using the  $SU(3)$  dynamical symmetries of the Interacting Boson Model-1 (IBM-1). Furthermore, the potential energy surfaces for these isotopes are plotted as functions of the deformation parameters  $\beta$  and  $\gamma$ . Moreover, we introduce empirical fit formulas for rotational and vibrational energies, which used to calculate these energies for the thorium isotopes. The obtained results by applying the IBM-1 and the authors' formulas are in good agreement with the corresponding experimental data for most of the nuclear states.

**In (2018) [32] Imad Mamdouh Ahmed *et al***, studying investigation of even–even  $^{220-230}\text{Th}$  isotopes within the IBM, IVBM and BM, and it found The properties of  $^{220-230}\text{Th}$  isotopes were studied and its energy states calculated. To identify the properties of each isotope, the values of the first excited states  $E2_1^+$  and the ratio of the second excited state to the first excited state  $R_{4/2} = E4_1^+/E2_1^+$  were adopted After identifying the properties of each isotope, the appropriate limit in the interacting boson model IBM-1, the IVBM model and the Bohr and Mottelson model were used to calculate the energy states for each isotope and compared the results with the experimental values

**In (2020)[33] K. Nomura *et al***, studied octupole correlations in light actinides from the interacting boson model based on the Gogny energy density functional and it found The quadrupole-octupole coupling and the related spectroscopic properties have been studied for the even-even light actinides  $^{218-238}\text{Ra}$  and  $^{220-240}\text{Th}$ . The diagonalization of the mapped IBM Hamiltonian provides energies for positive- and negative-parity states as well as wave functions which are employed to obtain transitional strengths. The results of the calculations compare well with available data from Coulomb excitation experiments and point towards a pronounced octupole collectivity around  $^{224}\text{Ra}$  and  $^{226}\text{Th}$ .

**In (2022)[34] Yu-Qing Wu *et al***, the energy dependence of the spectral fluctuations in the interacting boson model IBM and its connections to the mean-field structures have been analyzed through adopting two statistical measures. Specifically, the statistical results as functions of the energy cutoff have been worked out for different dynamical situations including the U(5)-SU(3) and SU(3)-O(6) transitions. It is found that most of the changes in

spectral fluctuations are triggered near the stationary points of the classical potential especially for the cases in the deformed region of the IBM phase diagram. The results thus justify the stationary point effects from the point of view of statistics.

## 1.5 The Aim of the Research

The aim of the work is studying properties of nuclei and know the nuclear structure of  $^{224-234}\text{Th}$  isotopes by:

1. Studying the energy levels of thorium isotopes ( $^{224-234}\text{Th}$ ) using the first interacting bosons model (IBM - 1) and determining the parameters used in this model and comparing the results with practical energy levels.
2. Calculating the value of reduced probability of electric transition  $B(E2)$  and comparing them with the experimental results.
3. Determine the value of the electric quadrupole moment  $Q$  responsible for determining the shape of the core and the amount of distortion that occurs in it.
4. Study and describe the nuclear structure of thorium isotopes using surface potential energy  $V(\beta, \gamma)$ .
5. Study the relation shape between the number of neutron with the deformation.

## Chapter Two

### *Interacting Boson Model (IBM-1)*

#### 2.1 Interacting boson model

After the previous nuclear models showed their inability to detect and determine some nuclear properties and the inconsistency of some of their results with the practical results obtained from the study of nuclear interactions, (Iachello and Arima) [5] in 1974 proposed a new nuclear model that combines the shell model and other models. This model was able to describe the characteristics of the lower aggregate levels (Low Lying Collective Levels) in even neutron and even atomic number nuclei.[35]

The basic rules of this model are built on some of the concepts and foundations that were applied in previous nuclear models as well as benefiting from the experimental results and depending on the mutual effect between nucleons caused by the strength of the pairing interaction between similar particles in addition to the strength of the quadrupole interaction between the asymmetric particles [36].

Accordingly, the nucleons outside the closed shells behave in the form of pairs that interact with each other, forming bosons, which have the ability to interact with each other, and can occupy the ground level (Ground State) when the angular momentum is equal to zero ( $L = 0$ ) and is called with (s-boson) or occupy the planes of excitable states when angular momentum is ( $L=2$ ) called (d-bosons) [37], or when ( $L=3$ ) bosons called (f-bosons), which describe symmetric states negative parity states [38].

## 2.2 IBM-1 Hamiltonian

Interacting boson model (IBM-1) has described collective features of even-even nuclei using interaction s-bosons and d-bosons [39],  $s^\dagger$ ,  $\tilde{s}$ ,  $d^\dagger$ , and  $\tilde{d}$  creation and annihilation operators define IBM, a six-dimensional Hilbert space.

This notion represents Low-lying collective states of even-even nuclei are N boson states. proton- and neutron-boson degrees of freedom are not separated in the IBM-1 model's original iteration[40].

Equation gives IBM-1 Hamiltonian forms (2.1)[41] :

$$\begin{aligned}
 \hat{H} = E_0 + \varepsilon_s (s^\dagger \cdot \tilde{s}) + \varepsilon_d (d^\dagger \cdot \tilde{d}) + \sum_{L=0,2,4} \frac{1}{2} (2L+1)^{\frac{1}{2}} C_L \left[ [d^\dagger \times d^\dagger]^{(L)} \times [\tilde{d} \times \tilde{d}]^{(L)} \right]^{(0)} + \frac{1}{\sqrt{2}} v_2 \left[ [d^\dagger \times d^\dagger]^{(2)} \times [\tilde{d} \times \tilde{s}]^{(2)} + [d^\dagger \times s^\dagger]^{(2)} \times [\tilde{d} \times \tilde{d}]^{(2)} \right]^{(0)} + \frac{1}{2} v_0 \left[ [d^\dagger \times d^\dagger]^{(0)} \times [\tilde{s} \times \tilde{s}]^{(0)} + [s^\dagger \times s^\dagger]^{(0)} \times [\tilde{d} \times \tilde{d}]^{(0)} \right]^{(0)} + u_0 \left[ [s^\dagger \times s^\dagger]^{(0)} + [\tilde{s} \times \tilde{s}]^{(0)} \right]^{(0)} + \frac{1}{2} u_2 \left[ [d^\dagger \times s^\dagger]^{(2)} \times [\tilde{d} \times \tilde{s}]^{(2)} \right]^{(0)} \quad (2.1)
 \end{aligned}$$

where  $(s^\dagger, \tilde{s})$  and  $(d^\dagger, \tilde{d})$  are the operators for creating and annihilating (s) and (d) bosons, respectively . Two of the nine Hamiltonian parameters are one-body terms ( $\varepsilon_s$ ,  $\varepsilon_d$ ) seven two-body terms, [ $C_L$  ( $L = 0,2,4$ ),  $v_L$  ( $L = 0,2$ ), and  $u_L$  ( $L = 0,2$ )].( $\varepsilon_s$ ) and ( $\varepsilon_d$ ) are the ( $C_l$ ), ( $v_l$ ), and ( $u_l$ ) have been used to describe the energies of single bosons and their interactions in pairs. This indicates that when the number of bosons (N) is

fixed, one one-body term and five two-body words are independent. This can be observed by considering ( $N = n_s + n_d$ ) [42,43].

Equation (2.2) groups the multipole expansion of the Hamiltonian of the IBM-1 into various boson-boson interactions, which is a more typical approach [7, 44]:

$$\hat{H} = \varepsilon \hat{n}_d + a_0 \hat{P}^\dagger \cdot \hat{P} + a_1 \hat{L}^\dagger \cdot \hat{L} + a_2 \hat{Q}^\dagger \cdot \hat{Q} + a_3 \hat{T}_3^\dagger \cdot \hat{T}_3 + a_4 \hat{T}_4^\dagger \cdot \hat{T}_4 \quad (2.2)$$

The equations define the operators.

$$\hat{n}_d = [d^\dagger \cdot \tilde{d}] \quad \text{the number of } d \text{ bosons}$$

$$\hat{P} = \frac{1}{2} (\tilde{d} \cdot \tilde{d}) - \frac{1}{2} (\tilde{s} \cdot \tilde{s}) \quad \text{the pairing operator for } d \text{ and } s \text{ bosons}$$

$$\hat{L} = \sqrt{10} [d^\dagger \times \tilde{d}]^{(1)} \quad \text{angular momentum operator}$$

$$\hat{Q} = [d^\dagger \times \tilde{s} + s^\dagger \times \tilde{d}]^{(2)} + \chi [d^\dagger \times \tilde{d}]^{(2)} \quad \text{quadrupole operator}$$

where  $\chi$  quadrupole structural parameter is 0 to  $\pm\sqrt{7}$  [43].

$$\hat{T}_3 = [d^\dagger \times \tilde{d}]^{(3)} \quad \text{the operator of octupole}$$

$$\hat{T}_4 = [d^\dagger \times \tilde{d}]^{(4)} \quad \text{the operator of hexapole}$$

$$\varepsilon = \varepsilon_d - \varepsilon_s \quad \text{the boson energy}$$

$\varepsilon$  have ( $\Delta n_d = 0$ ), while ( $\hat{P}^\dagger \cdot \hat{P}$ ) has ( $\Delta n_d = 0, \pm 2$ ) and ( $\hat{Q}^\dagger \cdot \hat{Q}$ ) has ( $\Delta n_d = 0, \pm 1, \pm 2$ ). The parameters dictated boson pairing, angular momentum, quadrupole, octupole, and hexadecapole interaction strength,  $a_0$ ,  $a_1$ ,  $a_2$ ,  $a_3$  and  $a_4$  respectively [7].

The IBM Hamiltonian provides precise solutions under three dynamical symmetry restrictions [U(5), O(6), and SU(3)], which geometrically resemble a harmonic vibrator, axial rotor, and  $\gamma$ -unstable rotor.

The Hamiltonian is an invariant operator of that chain of symmetries, causing a form phase transition between dynamical symmetry limits [7,45].

### 2.3 Electric Transitions

Along with agitation energy spectra, IBM has also described electric transition rates [46]. The absolute transition rates serve as a rigorous test for various theories in addition to being a sensitive aspect of nuclear structure. The majority of B(E2) values that are currently known were measured using coulomb excitation[47,48].

The following is a possible representation of the electromagnetic transition rates operators' general form [49]:

$$\hat{T}_m^l = \alpha_2 \delta_{l_2} [d^\dagger \times \tilde{s} + s^\dagger \times \tilde{d}]_m^2 + \beta_l [d^\dagger \times \tilde{d}]_m^l + \gamma_0 \delta_{l_0} \delta_{m_0} [s^\dagger \times \tilde{s}]_0^0 \quad (2.3)$$

where :  $l=0,1,2,3,4,\dots$ ;  $m=0,1,2,3,4,\dots$ , and  $\gamma_0, \alpha_2, \beta_l$  indicate the particular form of the transition operator and are parameters that specify the different terms in the related operators[50]. The electric quadrupole transition operators are as follows[51]:

$$\hat{T}_m^{(E2)} = \alpha_2 [d^\dagger \tilde{s} + s^\dagger \tilde{d}]_m^{(2)} + \beta_2 [d^\dagger \tilde{d}]_m^{(2)} \quad (2.4)$$

The magnetic dipole transition operator for d- bosons is described by the formula below [52]:

$$\hat{T}^{(M1)} = \beta_1 [d^\dagger \times \tilde{d}]_m^{(1)} \quad (2.5)$$

B(EL),B(ML) is the reduced transition probability formula for electric and magnetic transitions [53]:

$$B(L, I_i \rightarrow I_f) = \frac{1}{2I_i + 1} |\langle I_i || \hat{T}^L || I_f \rangle|^2 \quad (2.6)$$

where  $|\langle I_i || \hat{T}^L || I_f \rangle|$  is the matrix element of (E2) transition.

## 2.4 Dynamical Symmetries

The dynamic symmetries are utilized to resolve problems of the Eigen values in Hamiltonian operators [5], Bosons in the model of interacting bosons (IBM-1) have six-dimensional space because of they have six sub-levels like a outcome they could be characterized in the form of unitary group which illustrated by U(6), this could be resolved to three dynamical symmetries [54].

The three limits, or symmetries, of the IBM are called the U(5), SU(3) and O(6) limits and correspond to the vibrational, rotational, and  $\gamma$ -unstable nuclear structures, respectively.

The first group, U(6) is represented by the quantum number, N (total number of bosons), and so all states in the U(6) group are degenerate. Each step of the group chain introduces a unique quantum number and breaks the degeneracy of the previous group, except for the  $(n_\Delta)$  and  $(\nu_\Delta)$  terms. The degeneracy is broken until the O(3) group is reached.

The  $(n_\Delta)$  and  $(\nu_\Delta)$  quantum numbers are labels to distinguish between degenerate states and are related to the number of boson triplets coupled to spin 0.

Equation (2.11) can be formulated as follow [54]:

$$\hat{H} = \sum_{i=1}^N \varepsilon_i + \sum_{i<j}^N V_{ij} \quad (2.7)$$

where as  $(\varepsilon_i)$  is the energy of bosons and  $(N)$  represents the number of bosons and finally  $(V_{ij})$  depicts the interaction effort between bosons.

### 2.4.1 Vibrational Limit of the IBM-1 $U(5)$

The dynamic symmetry of the Hamiltonian factor can be calculated using the equation below[55]:

$$\hat{H} = \varepsilon \hat{n}_d + a_1 \hat{L} \cdot \hat{L} + a_3 \hat{T}_3 \cdot \hat{T}_3 + a_4 \hat{T}_4 \cdot \hat{T}_4 \quad (2.8)$$

In this limit, the operators  $(\hat{P})$  and  $(\hat{Q})$  are obviously inefficient, as shown in equation (2.7). The Hamiltonian operator's eigen value equation is given in the formula below [56] :

$$E = \varepsilon_{n_d} + \alpha \frac{1}{2} n_d (n_d - 1) + \beta (n_d - \nu) (n_d + \nu + 3) + \gamma [L(L + 1) - 6n_d] \quad (2.9)$$

$U(5)$  and its quantum numbers indicate vibrational dynamical symmetry[53]:

$$\left| \begin{array}{ccccc} U(6) \supset & U(5) & \supset & O(5) & \supset & O(3) & \supset & O(2) \\ \downarrow & \downarrow & & \downarrow & & \downarrow & & \downarrow \\ [N] & n_d & & \nu, n_\Delta & & L & & M \end{array} \right. \quad (2.10)$$

$N$  is the total boson count,  $n_d$  is the number of d-bosons, and  $(\nu)$  is the seniority, which is used to calculate the number of d-bosons that aren't pairwise coupled with  $(L=0)$ . The number of tripled d-bosons associated

with (L=0) and (L,M), the two quantum numbers used to represent the angular momentum and components, is known as  $n_{\Delta}$  [57]. A typical spectrum for the U(5) limit is shown in figure (2.1).

The reduce transition probabilities for the electric quadruple are determined using the following formula [58]:

$$B(E2; L + 2 \rightarrow L) = \frac{\alpha_2^2}{4} (L + 2)(2N_{\rho} - L) \quad (2.11)$$

For the ground state

$$B(E2; 2_1^+ \rightarrow 0_1^+) = \alpha_2^2 N_{\rho} \quad (2.12)$$

The following formula can be used to express the quadruple momentum [59]:

$$Q_L = \beta_2 \sqrt{\frac{16\pi}{5}} \sqrt{\frac{1}{14}} L \quad (2.13)$$

$$Q_{2_1^+} = \beta_2 \sqrt{\frac{16\pi}{5}} \sqrt{\frac{2}{7}} \quad \text{For } 2_1^+ \text{ state} \quad (2.14)$$

$$\text{where, } \beta_2 = -\frac{0.7}{\sqrt{2}} \alpha_2 \quad (2.15)$$

The equation below gives the branching ratio  $R, R'$  and  $R''$  for U(5) limit [60]:

$$R = \frac{B(E2; 4_1^+ \rightarrow 2_1^+)}{B(E2; 2_1^+ \rightarrow 0_1^+)} = 2 \frac{(N_{\rho} - 1)}{N} \leq 2 \quad (2.16)$$

$$R' = \frac{B(E2; 2_2^+ \rightarrow 2_1^+)}{B(E2; 2_1^+ \rightarrow 0_1^+)} = 2 \frac{(N_{\rho} - 1)}{N} \leq 2 \quad (2.17)$$

$$R'' = \frac{B(E2; 0_2^+ \rightarrow 2_1^+)}{B(E2; 2_1^+ \rightarrow 0_1^+)} = 2 \frac{(N_{\rho} - 1)}{N} \leq 2 \quad (2.18)$$

Figure (2.1) depicts an ideal energy spectrum using the quantum number  $n_d$  from dynamical symmetry U(5).

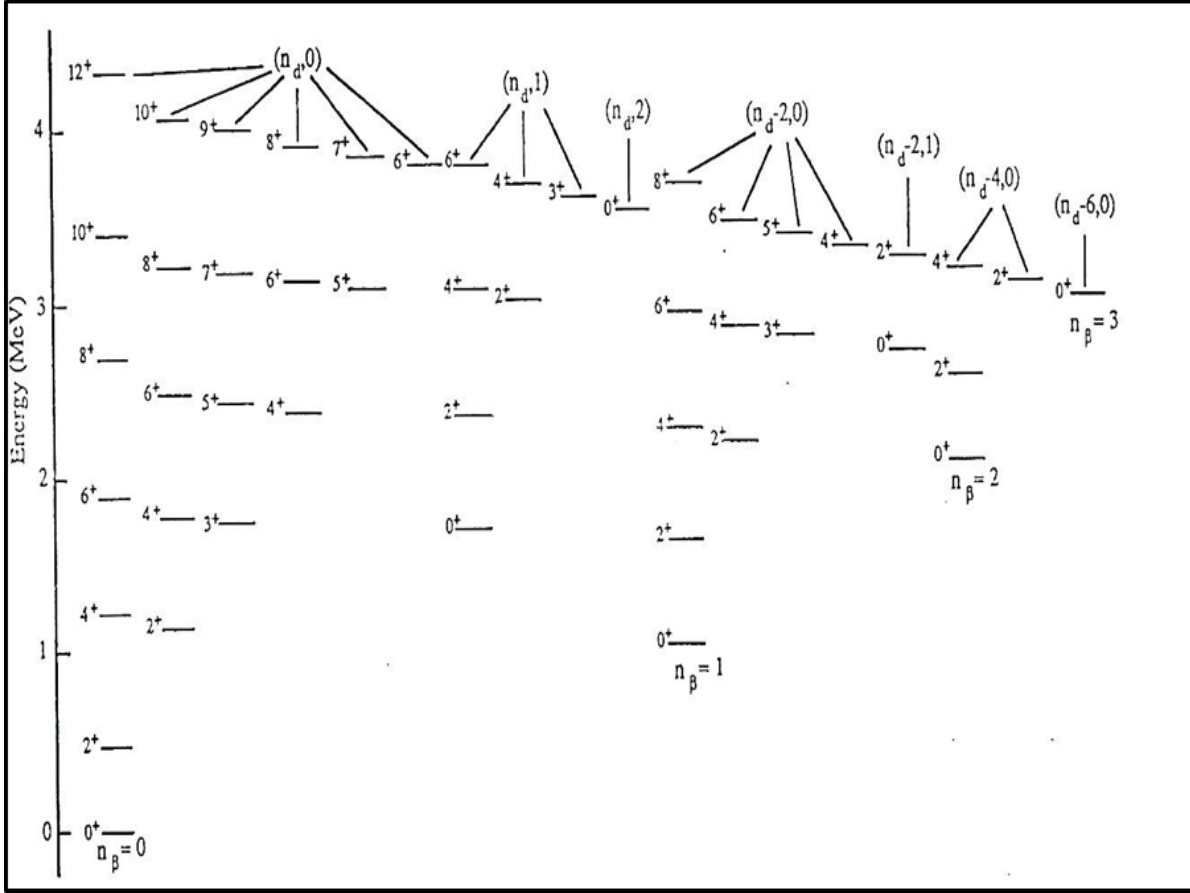


**Figure (2.1):** A typical spectrum and a quantum numbers for U(5) symmetry [61].

### 2.4.2 Rotational Limit of the IBM-1 $SU(3)$

The Hamiltonian for dynamical symmetry can be written as creation and annihilation operators in the rotating limit subgroup  $SU(3)$  [62], as seen in the equation below, which only has variables  $a_1$  and  $a_2$  [63]:

$$\hat{H} = a_1 \hat{L}\hat{L} + a_2 \hat{Q}\hat{Q} \quad (2.19)$$

In this limit, the operators  $(\varepsilon, \hat{P}, \hat{T}_3$  and  $\hat{T}_4)$  are ineffectual [64]. The Eigen value for this dynamical [65] is:

$$E = \frac{a_2}{2} [\lambda^2 + \mu^2 + \lambda\mu + 3(\lambda + \mu)] + \left( a_1 - \frac{3a_2}{8} \right) L(L + 1) \quad (2.20)$$

The quantum numbers shown in the eigen value equation can be represented by the degenerate chain SU(3) [66]:

$$\left| \begin{array}{cccc} U(6) \supset & SU(3) \supset & O(3) \supset & O(2) \\ \downarrow & \downarrow & \downarrow & \downarrow \\ [N] & (\lambda, \mu)K & L & M \end{array} \right| \quad (2.21)$$

where (K) represents the number of cases with equal values of  $(\lambda, \mu, L)$ , and the quantum numbers  $(\lambda, \mu)$  represent cases SU(3), the equation below shows operator (E2) [67]:

$$T_m^{(E2)} = \alpha_2 \left[ (d^\dagger \tilde{s} + s^\dagger \tilde{d})_m^{(2)} - \frac{\sqrt{7}}{2} (d^\dagger \tilde{d})_m^{(2)} \right] \quad (2.22)$$

$$\text{where, } \beta_2 = -\frac{\sqrt{7}}{2} \alpha_2 \quad (2.23)$$

The selection rules in this limit are :

$$\Delta\lambda = 0, \Delta\mu = 0$$

The value of  $B(E2)$  follows formula :

$$B(E2; L + 2 \rightarrow L) = \alpha_2^2 \frac{3}{4} \frac{(L+2)(L+1)}{(2L+3)(2L+5)} (2N_\rho - L)(2N_\rho + L + 3) \quad (2.24)$$

For ground state:

$$B(E2; 2_1^+ \rightarrow 0_1^+) = \alpha_2^2 \frac{1}{5} N_\rho (2N_\rho + 3) \quad (2.25)$$

For this limit, the electric quadrupole momentum is given [68]:

$$Q_L = -\alpha_2 \sqrt{\frac{16\pi}{40}} \frac{L}{2L+3} (4N+3) \quad (2.26)$$

As  $Q_{2_1^+}$  becomes ;

$$Q_{2_1^+} = -\alpha_2 \sqrt{\frac{16\pi}{40}} \frac{2}{7} (4N+3) \quad (2.27)$$

The branching ratios  $R, R'$  and  $R''$  for SU(3) limit can be deduced from [44]:

$$R = \frac{B(E2; 4_1^+ \rightarrow 2_1^+)}{B(E2; 2_1^+ \rightarrow 0_1^+)} = \frac{10(N_\rho-1)(2N_\rho+5)}{7N_\rho(2N_\rho+3)} \leq \frac{10}{7} \quad (2.28)$$

$$R' = \frac{B(E2; 2_2^+ \rightarrow 2_1^+)}{B(E2; 2_1^+ \rightarrow 0_1^+)} = 0 \quad (2.29)$$

$$R'' = \frac{B(E2; 0_2^+ \rightarrow 2_1^+)}{B(E2; 2_1^+ \rightarrow 0_1^+)} = 0 \quad (2.30)$$

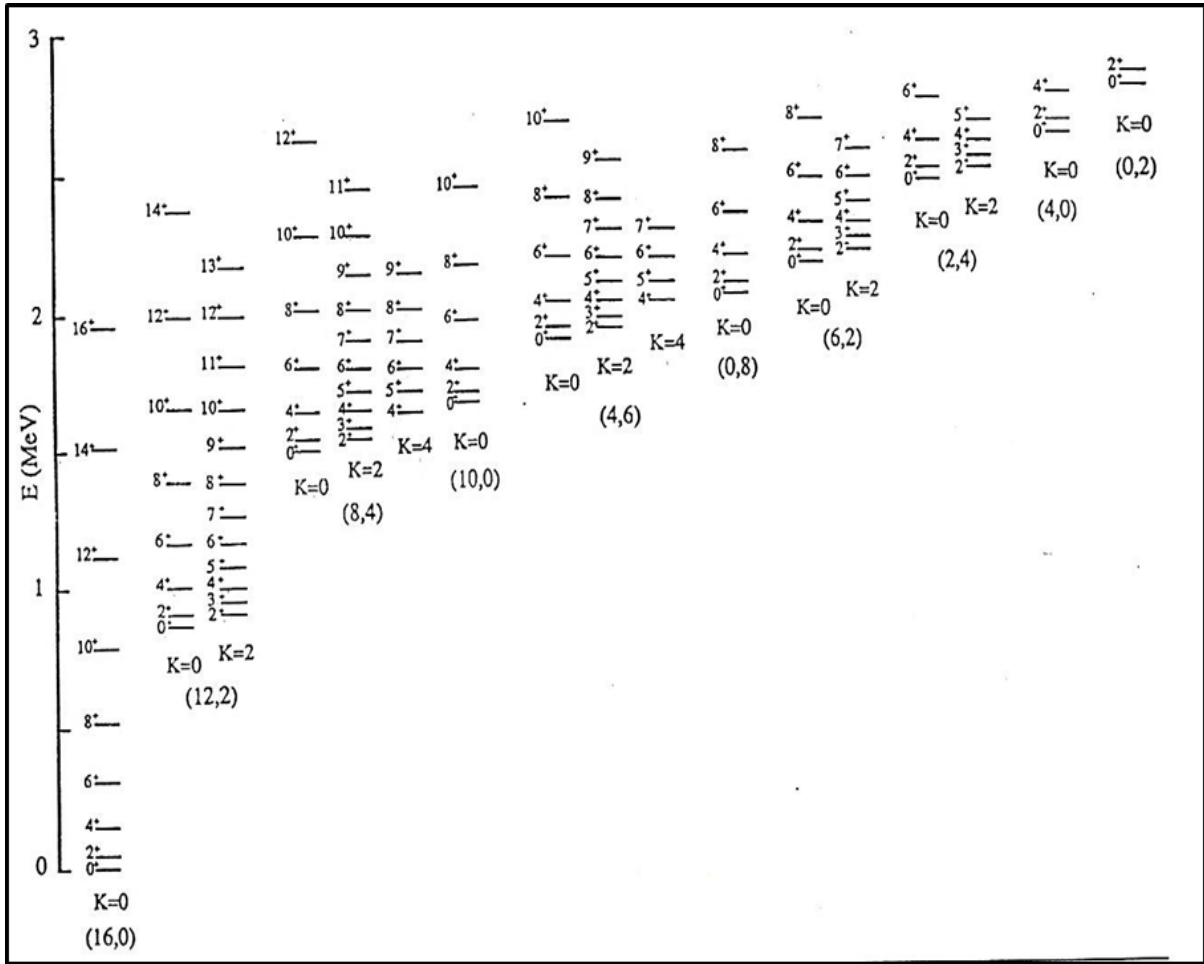


Figure (2.2): A typical spectrum and a quantum numbers for SU(3) symmetry[68]

### 2.4.3 $\gamma$ -Unstable Limit of the IBM-1 O(6)

This limit is created when the energy of bosons ( $\epsilon$ ) is dominated by the interaction coupling ( $\hat{P} \cdot \hat{P}$ ) between bosons [69]. the Hamiltonian operators in this case [69]:

$$\hat{H} = a_0 \hat{P} \cdot \hat{P} + a_1 \hat{L} \cdot \hat{L} + a_3 \hat{T}_3 \cdot \hat{T}_3 \quad (2.31)$$

The dynamical eigenvalue equation is presented in [70]:

$$E = A \frac{1}{4} (N_\rho - \sigma)(N_\rho + \sigma + 4) + B \frac{1}{6} \tau(\tau + 3) + CL(L + 1) \quad (2.32)$$

The quantum numbers for the unstable gamma represented by the sub-group O(6) can be represented by the equation

$$\left| \begin{array}{ccccccccc} U(6) & \supset & O(6) & \supset & O(5) & \supset & O(3) & \supset & O(2) \\ \downarrow & & \downarrow & & \downarrow & & \downarrow & & \downarrow \\ [N] & & \sigma & & \tau, \nu_{\Delta} & & L & & M \end{array} \right| \quad (2.33)$$

$\sigma, \tau$ : is a quantum numbers which is given as follows:

$$\sigma = N_{\rho}, N_{\rho} - 2, \dots, 0 \text{ or } 1, \text{ for } N_{\rho} = \text{even or odd.}$$

$$\tau = 0, 1, \dots, \sigma.$$

where ( $A = \frac{a_0}{4}$ ,  $B = \frac{a_3}{2}$  and  $C = \frac{a_1 - a_3}{10}$ ) which represent the conjugate eigen value and ( $\nu_{\Delta}$ ) represents is number of  $d$ - bosons tripled coupled with zero angular momentum[70-71]. Figure (2.3) shows a typical spectrum to  $O(6)$  limit[56], the quadrupole transition operator( $T_m^{(E2)}$ ) is [72]:

$$T_m^{(E2)} = \alpha_2 [d^{\dagger} \tilde{s} + s^{\dagger} \tilde{d}]_m^{(2)}. \quad (2.34)$$

where ( $\beta_2 = 0$ ), and the selection rules are ( $\Delta\delta = 0, \Delta\tau = \pm 1$ ),  $B(E2)$  equals:

$$B(E2; L+2 \rightarrow L) = \alpha_2^2 \frac{(L+2)}{2(L+5)} \frac{1}{4} (2N_{\rho} - L)(2N_{\rho} + L + 8) \quad (2.35)$$

when  $L=0$  is:

$$B(E2; 2_1^+ \rightarrow 0_1^+) = \alpha_2^2 \frac{1}{5} N_{\rho} (N_{\rho} + 4) \quad (2.36)$$

Concludes from the selection rules that the value of quadrupole momentum equals zero:  $Q_L = 0$ .

The branching ratios  $R, R'$  and  $R''$  for the  $O(6)$  limit are given by the formulae below[43]:

$$R = \frac{B(E2; 4_1^+ \rightarrow 2_1^+)}{B(E2; 2_1^+ \rightarrow 0_1^+)} = \frac{10(N_\rho - 1)(N_\rho + 5)}{7N_\rho(N_\rho + 4)} < \frac{10}{7} \quad (2.37)$$

$$R' = \frac{B(E2; 2_2^+ \rightarrow 2_1^+)}{B(E2; 2_1^+ \rightarrow 0_1^+)} = \frac{10(N_\rho - 1)(N_\rho + 5)}{7N_\rho(N_\rho + 4)} < \frac{10}{7} \quad (2.38)$$

$$R'' = \frac{B(E2; 0_2^+ \rightarrow 2_1^+)}{B(E2; 2_1^+ \rightarrow 0_1^+)} = 0 \quad (2.39)$$

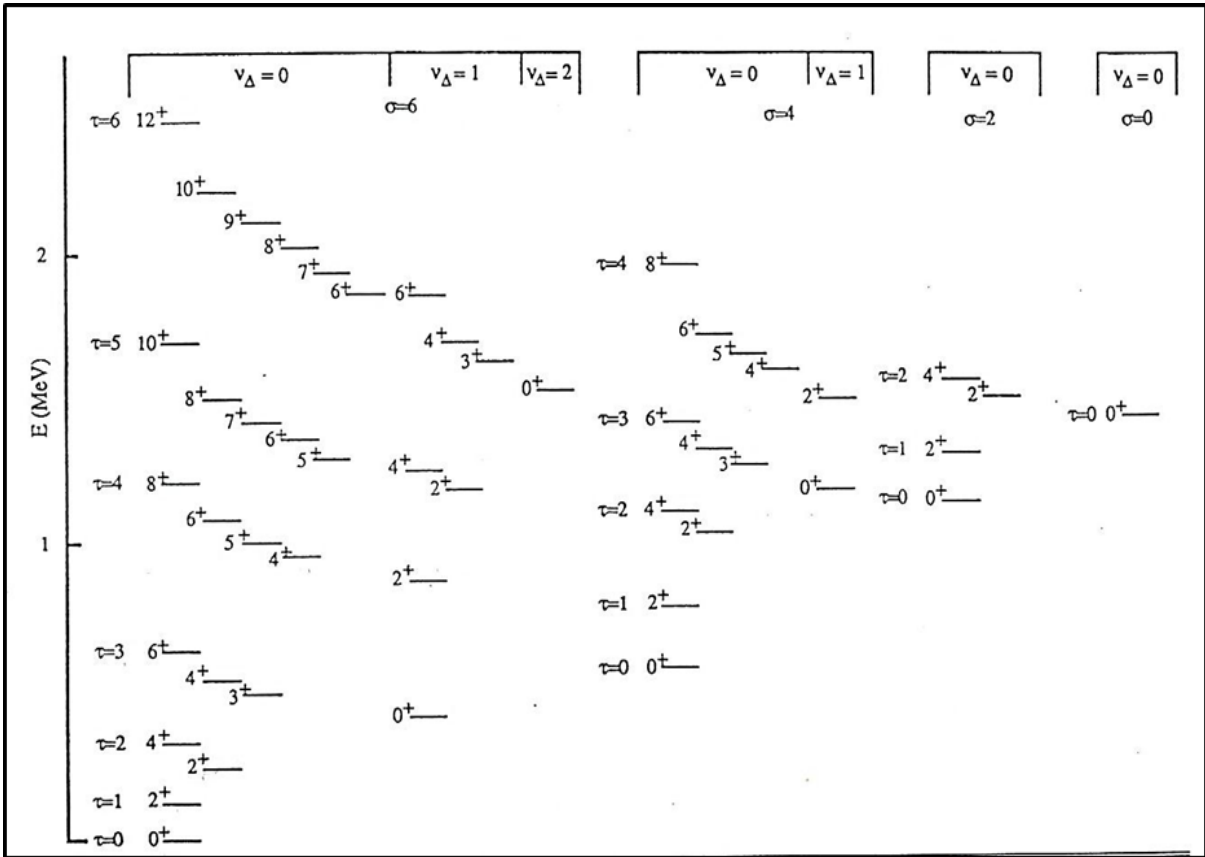
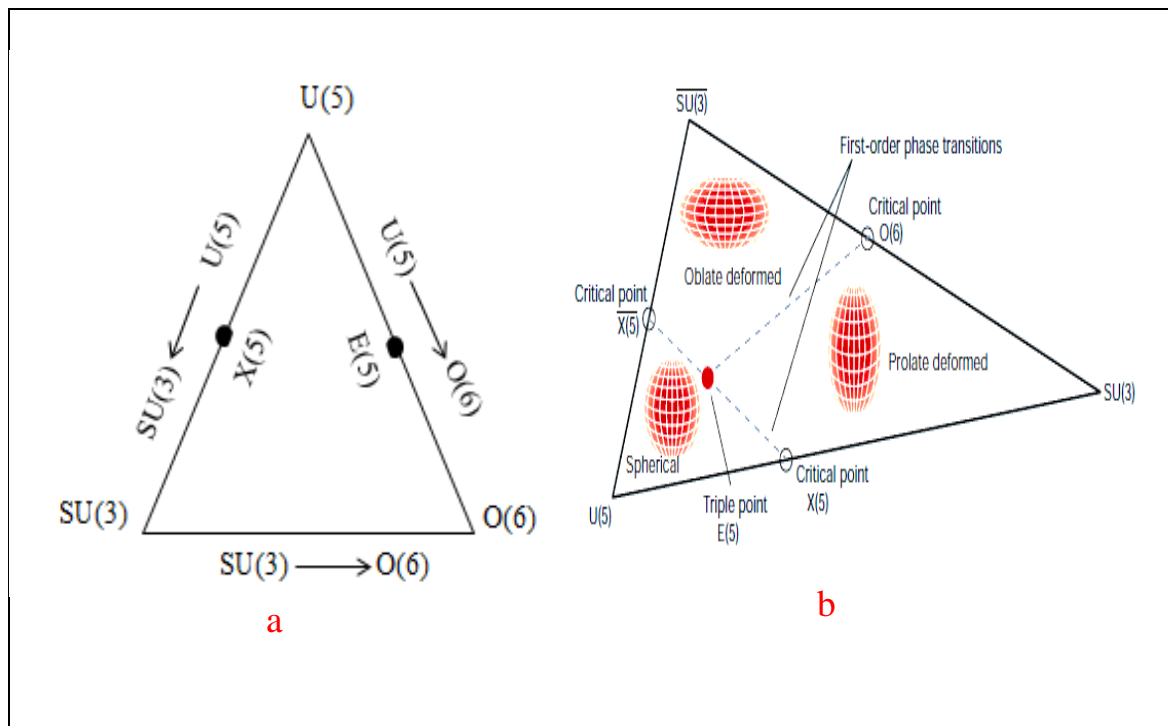


Figure (2.3) A typical spectrum and a quantum numbers for O(6) symmetry [73].

## 2.5 Transitional Regions in IBM

The dynamical symmetries in the triangle's vertices, which are at the termini of the transition leg [74,75], can represent many nuclei that transition between two or three boundaries. The Casten triangle, seen in

figure (2.4), exhibits three dynamical symmetries and transitional regions [76].



**Figure (2.4)** The Casten triangle

A mathematical symmetry that is identical to one of the three forms mentioned above is represented by each peak in figure (b). As first-order phase transitions, transition sites and their essential symmetries are defined. this suggests second-order transition. between a spherical and a prolate or oblate distorted nuclear shape, presuming that there is a nuclear triple point [76]. The limits previously discussed offer a set of analytical solutions that can be easily tested due to the small number of nuclei that may be characterized by these limitations and the fact that the majority of nuclei share similar characteristics between these limits, which are known as the transition area, which can be divided into four types [77]:

### 2.5.1 Type 1: $U(5) \rightarrow O(6)$

The characteristics of the nuclei are intermediate between those of the vibrational limit and the -unstable limit in this region of transition, and the Hamiltonian is [78]:  $(\varepsilon/a_0)$ ,

$$\hat{H} = \varepsilon \hat{n}_d + a_0 \hat{P} \cdot \hat{P} + a_1 \hat{L} \cdot \hat{L} + a_3 \hat{T}_3 \cdot \hat{T}_3 \quad (2.40)$$

when is big, the qualities of this limit tend to be vibrational, whereas when is small, the properties tend to be - unstable. The properties of this limit rely depend on the ratio  $(\varepsilon/a_0)$ .

### 2.5.2 Type 2: $O(6) \rightarrow SU(3)$

The nuclei's characteristics in the transition area lie between those of the rotating limit and the -unstable limit, and the Hamiltonian is [79]:

$$\hat{H} = a_0 \hat{P} \cdot \hat{P} + a_1 \hat{L} \cdot \hat{L} + a_2 \hat{Q} \cdot \hat{Q} \quad (2.41)$$

The ratio  $(a_0/a_2)$  governs the characteristics of nuclei in this region. Thus, the properties approach the  $O(6)$  limit as the ratio grows and the  $SU(3)$  limit as it lowers.

### 2.5.3 Type 3: $U(5) \rightarrow SU(3)$

The nuclei's properties in the transition region lie between the limits for vibration and rotation, and the Hamiltonian operator is as follows [80]:

$$\hat{H} = \varepsilon \hat{n}_d + a_1 \hat{L} \cdot \hat{L} + a_2 \hat{Q} \cdot \hat{Q} \quad (2.42)$$

The ratio  $(\varepsilon/a_2)$  governs the properties of nuclei in this region. As a result, as the ratio rises, the properties approach the  $U(5)$  limit, and as the ratio falls, they approach the  $SU(3)$  limit.

### 2.5.4 Type 4 : $U(5) \rightarrow SU(3) \rightarrow O(6)$

The Hamiltonian operator is stated as follows equation (2.43). The common characteristics between the three limits are shared by the nuclei of this type [81]:

$$\hat{H} = \varepsilon \hat{n}_d + a_0 \hat{P} \cdot \hat{P} + a_1 \hat{L} \cdot \hat{L} + a_2 \hat{Q} \cdot \hat{Q} + a_3 \hat{T}_3 \cdot \hat{T}_3 + a_4 \hat{T}_4 \cdot \hat{T}_4 \quad (2.43)$$

## 2.6 Surface Potential Energy

Equation (2.44) shows how the surface potential energy may be calculated from the Hamiltonian function's impact on energy counting, which depends on the total number of bosons (N) and the two distortion factors ( $\beta, \gamma$ ) :

$$E(N, \beta, \gamma) = \frac{\langle N, \beta, \gamma | H | N, \beta, \gamma \rangle}{\langle N, \beta, \gamma | N, \beta, \gamma \rangle} \quad (2.44)$$

The energy surface, as a function of ( $\beta$ ) and ( $\gamma$ ), has been given by:

$$V(N, \beta, \gamma) = \frac{N\varepsilon_d\beta^2}{(1+\beta^2)} + \frac{N(N+1)}{(1+\beta^2)^2} (a_1\beta^4 + a_2\beta^3 \cos 3\gamma + a_3\beta^2 + a_4) \quad (2.45)$$

Through studying the potential energy  $V(\beta, \gamma)$ , we can know the shape of the deformed nuclei, as  $\gamma$  represents the amount of deviation from the axis of symmetry, and takes values between ( $\gamma = 60, \gamma = 0$ ), while the variable  $\beta$  represents the amount of deviation from the spherical shape and takes values between ( $\beta = 2.4, \beta = 0$ ) [82]. The following equations represent the surface energy of the three symmetries: [38,82]

$$E(N, \beta, \gamma) \propto \begin{cases} \text{U(5):} & \varepsilon_d N \frac{\beta^2}{1 + \beta^2} \\ \text{SU(3):} & \frac{\frac{3}{4}\beta^4 - \sqrt{2}\beta^3 \cos 3\gamma + 1}{(1 + \beta^2)^2} \\ \text{O(6):} & k'N(N-1) \left( \frac{1 - \beta^2}{1 + \beta^2} \right)^2 \end{cases} \quad (2.46)$$

where (  $k \propto a_2$  and  $k' \propto a_0$  ) in Eq. (2.2).

Figure (2-5) represents the ideal scheme for contour lines and axial symmetries [83]

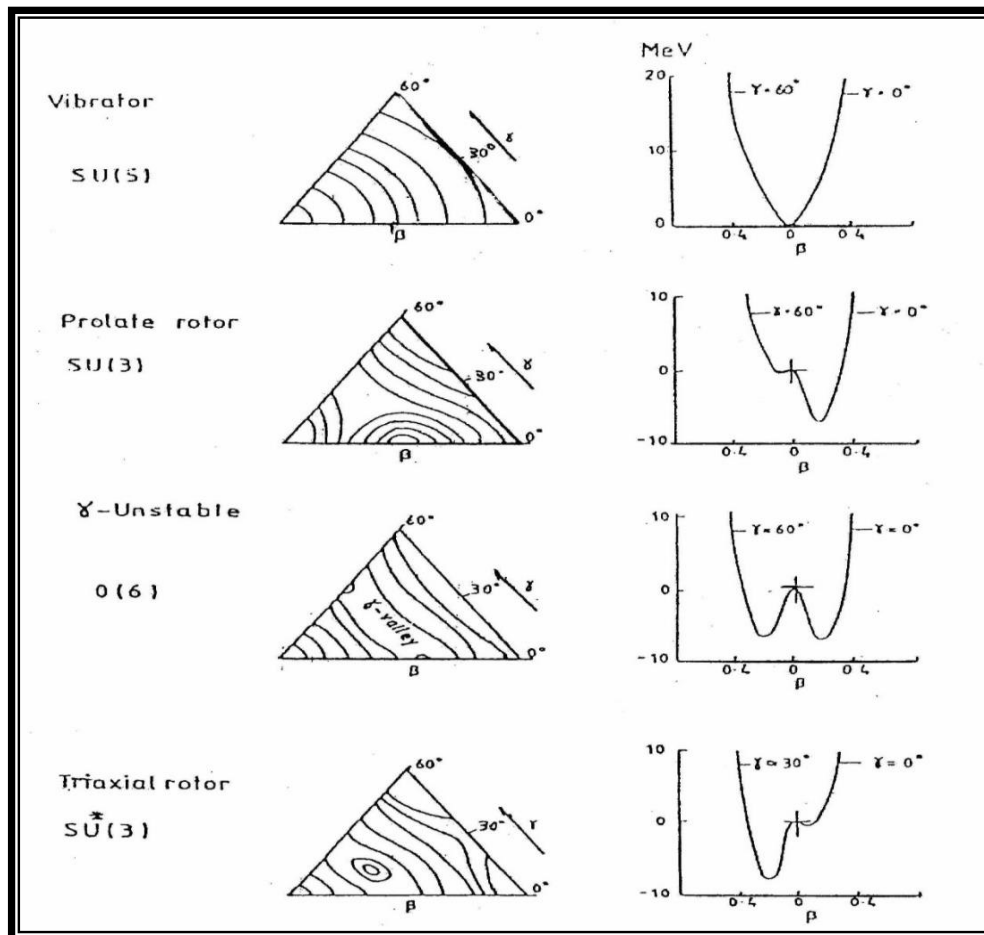


Figure (2.5): ideal scheme for potential energy surface [83]

## *chapter Three*

### *Results and Discussion*

#### **3.1 Introduction**

IBM-1 is used in this research to investigate a number of nuclear structure-related aspects for even-even  $^{224-234}\text{Th}$  isotopes, including reduced electric transition probabilities, dynamic symmetries, electric quadrupole moment values, energy level states low-lying positive parity states, surface of potential energy. These nuclei have limitations that range from SU(3), U(5) and O(6). Thorium isotopes have atomic number equal (90), which is near from (82) closed shell, then the protons bosons are (4). The neutrons number for these isotopes are between (134) and (144), which is near closed shell. As in table (3.1) shows the number of bosons  $N$  and protons  $N_{\pi}=4$  for all even-even  $^{224-234}\text{Th}$  and the number of neutrons bosons  $N_{\nu}=4$  to 9 for  $^{224-234}\text{Th}$ , respectively.

#### **3.2 Calculation Energy Levels:**

Estimating the parameters of the Hamiltonian dependent the experimental energy levels and the standard ratio between them as in table (3.1) for each limit.

Table (3.1) Energy ratios for each limit are typical. [34, 41]

Limit	$\frac{E_{4_1^+}}{E_{2_1^+}}$	$\frac{E_{6_1^+}}{E_{2_1^+}}$	$\frac{E_{8_1^+}}{E_{2_1^+}}$	$\frac{E_{0_2^+}}{E_{2_1^+}}$
$U(5)$	2	3	4	2
$SU(3)$	3.33	7	12	$\gg 2$
$O(6)$	2.5	4.5	7	4.5

These values were compared to experimental values from reference [66] and typical values for each limit [84,85], For even-even  $^{224-234}\text{Th}$  isotopes as in figures (3.1 - 3.3).

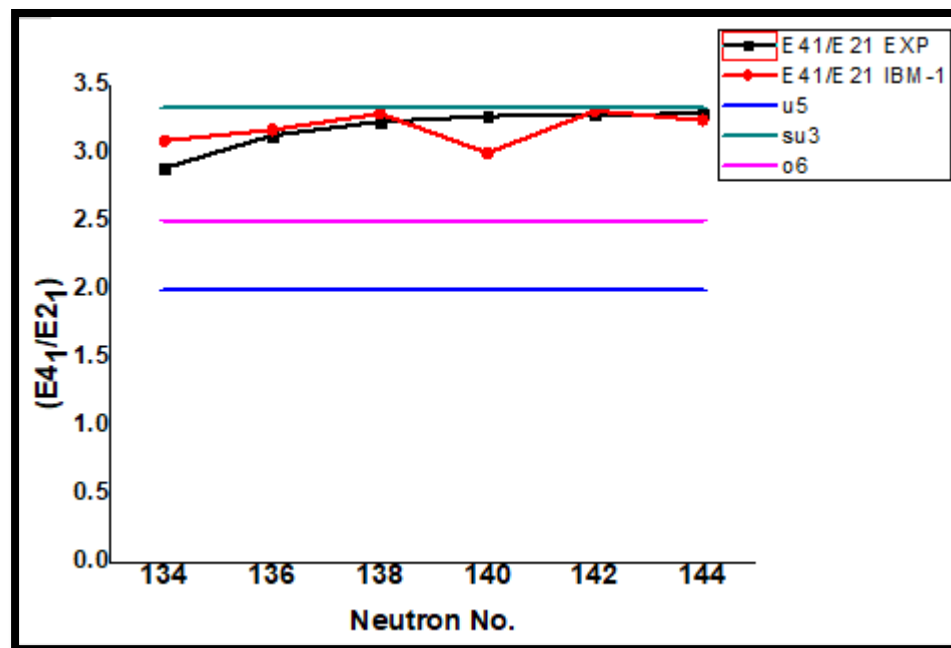


Figure (3.1) :The ratio  $E_{4_1^+}/E_{2_1^+}$  has been compared with experimental data.

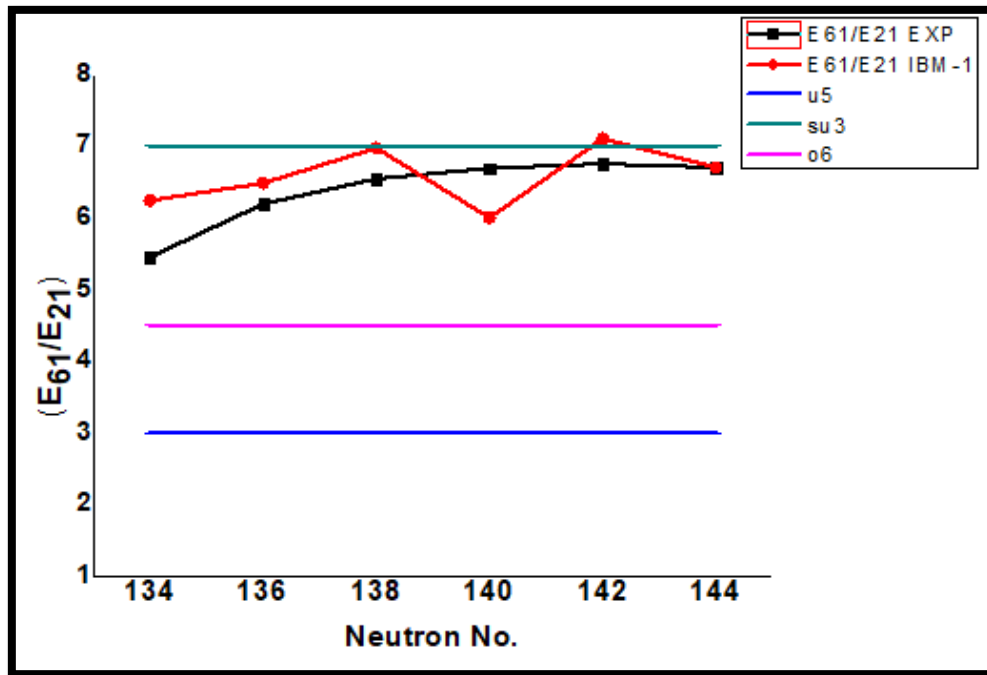


Figure (3.2) The ratio  $E_{61^+}/E_{21^+}$  has been compared with experimental data.

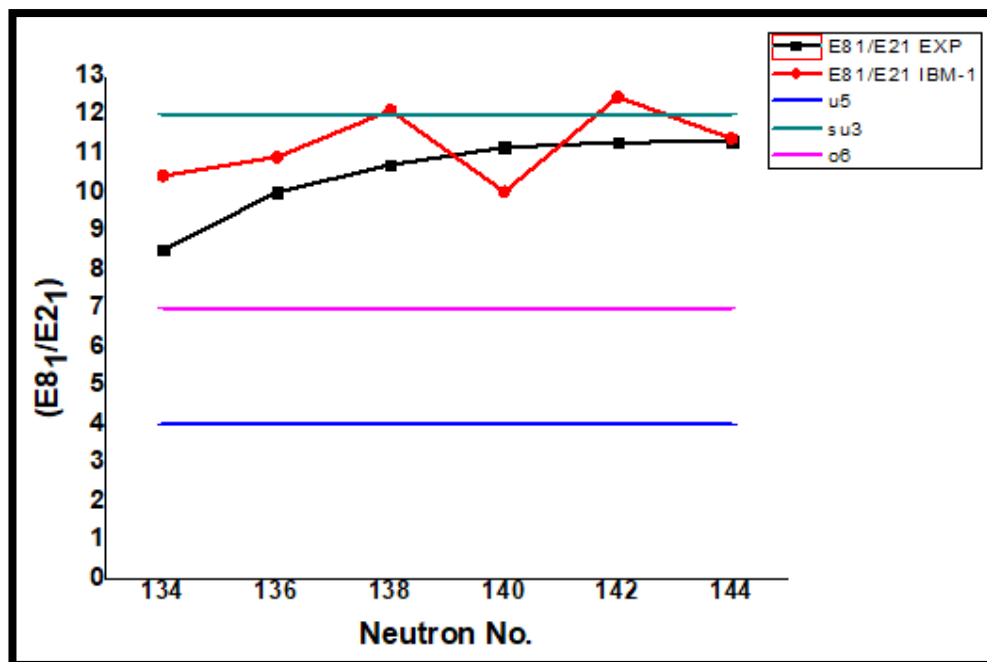


Figure (3.3) The ratio  $E_{81^+}/E_{21^+}$  has been compared with experimental data.

Figures (3.1-3.3), show that  $^{224}\text{Th}$ ,  $^{226}\text{Th}$  placed within transition limit between SU(3) and O(6), then  $^{228}\text{Th}$ ,  $^{230}\text{Th}$  and  $^{232}\text{Th}$  return to SU(3) limit. The last isotopes  $^{234}\text{Th}$  will be in limit O(6) and SU(3) but close to SU(3).

The values of the parameters of Hamilton in equation (2.2) that gave the best agreement with the experimental values [86-87] are shown in Table (3.2).

**Table (3.1):** values for Hamiltonian parameters as in IBM program.

The Isotopes	Boson number	E P S (MeV)	P . P (MeV)	L . L (MeV)	Q . Q (MeV)	T <sub>3</sub> . T <sub>3</sub> (MeV)	T <sub>4</sub> . T <sub>4</sub> (MeV)	CHI	SO6
$^{224}\text{Th}$	8	0.0000	0.0013	0.0082	-0.0102	0.0000	0.0000	-1.700	1
$^{226}\text{Th}$	9	0.0000	0.0013	0.0082	-0.0069	0.0000	0.0000	-1.700	1
$^{228}\text{Th}$	10	0.0000	0.0000	0.0008	-0.0242	0.0000	0.1500	-5.490	1
$^{230}\text{Th}$	11	0.0000	0.0000	0.0005	-0.0182	0.0000	0.1000	0.1250	1
$^{232}\text{Th}$	12	0.0000	0.0000	0.0005	-0.0200	0.0000	0.1500	0.5000	1
$^{234}\text{Th}$	13	0.0000	0.0025	0.0069	-0.0026	0.0000	0.0000	0.0900	1

Depending on equation (2.41), for transition region between SU(3) and O(6), estimating the Hamiltonian parameters for  $^{224}\text{Th}$  and  $^{226}\text{Th}$  as shown in table (3.2).

SU(3) pure limit as equation (2.19), applying for  $^{228}\text{Th}$ ,  $^{230}\text{Th}$  and  $^{232}\text{Th}$ , but not getting a good fitting unless addition limit which is T<sub>4</sub> and so called breaking

symmetry . Final isotope  $^{234}\text{Th}$ , is transition limit SU(3) and O(6) ,by applying equation (2.41)

Figures (3.4–3.9) compare theoretical and experimental energy levels using data from references [88]. For all of the nuclei under examination, The agreement between our computation for the ground-band and the actual results is very good, and a decent agreement for the other bands if there are data.

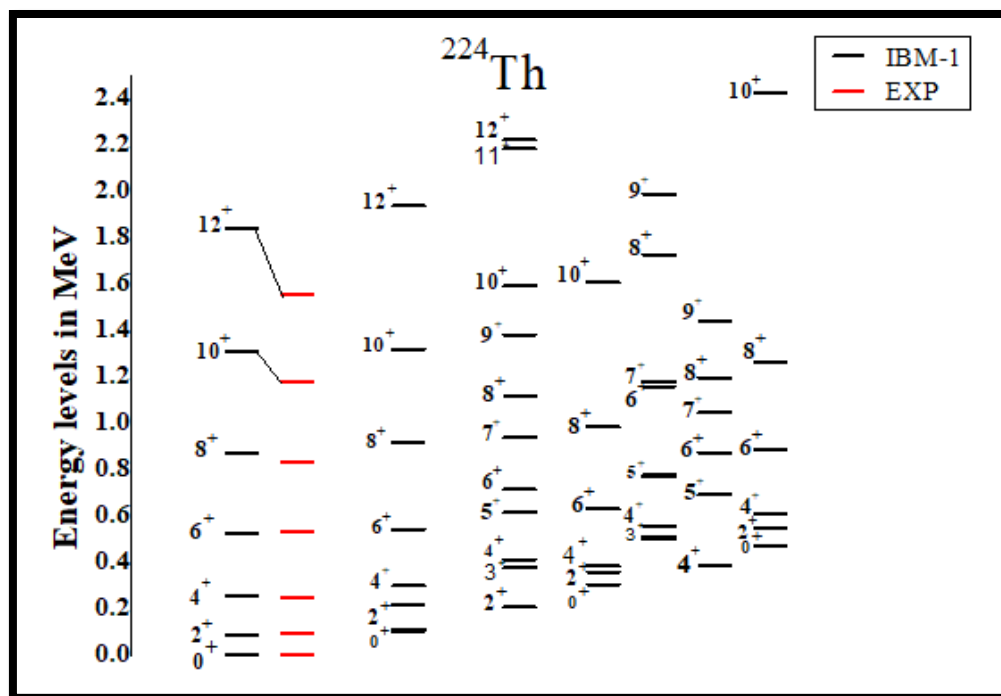


Figure (3.4) The arrangement of energy levels for  $^{224}\text{Th}$  , theoretical and experimental

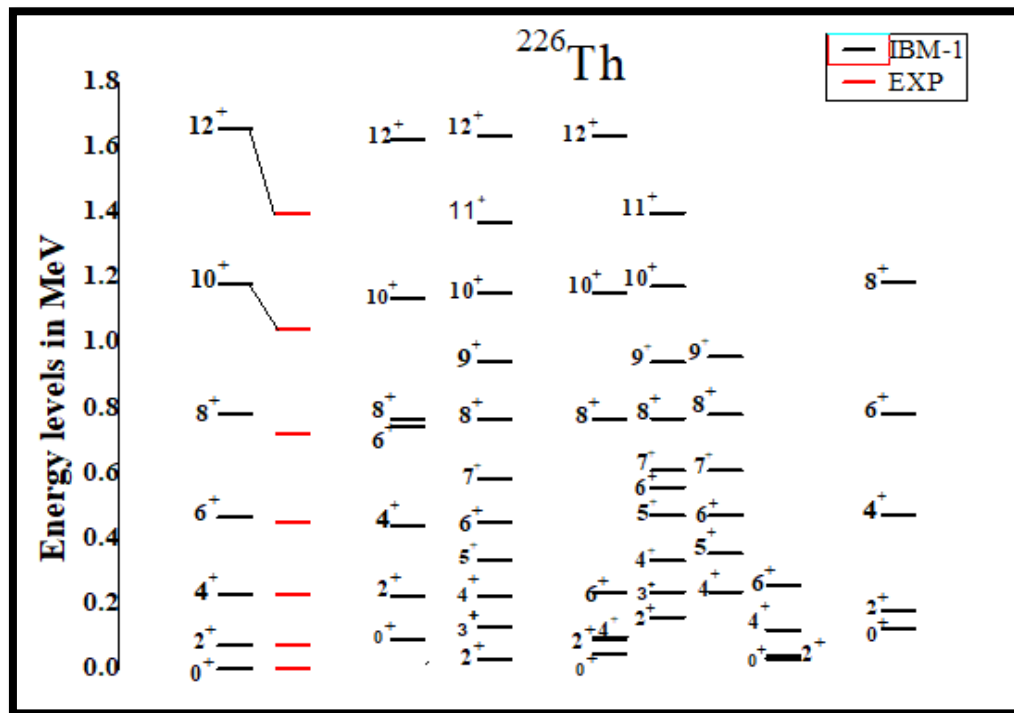


Figure (3.5) The arrangement of energy levels for  $^{226}\text{Th}$ , theoretical and experimental

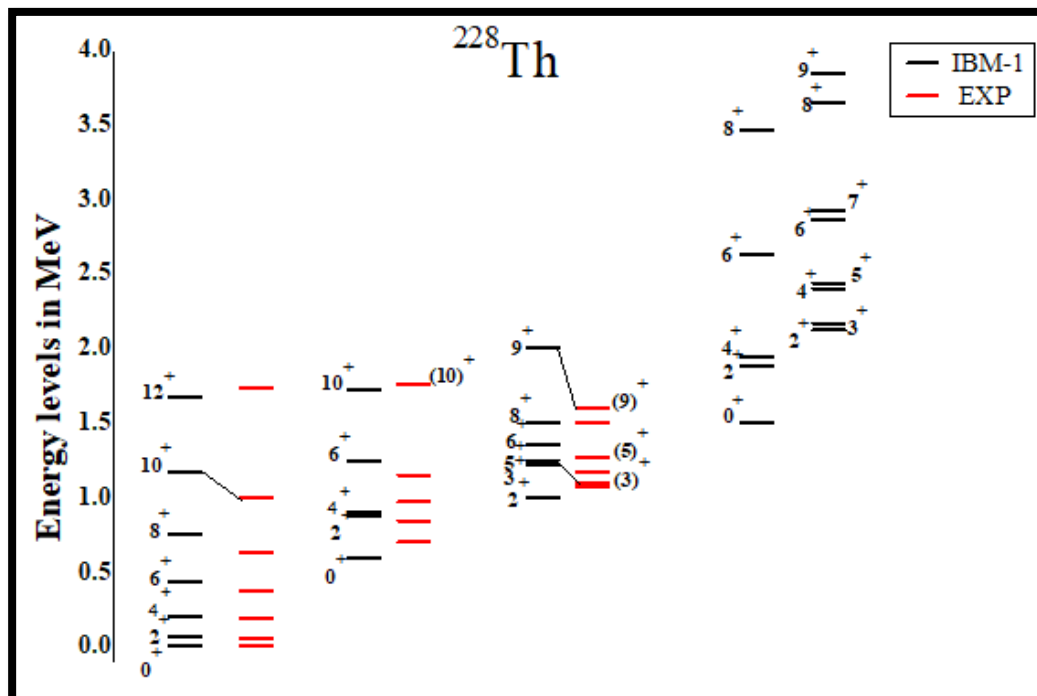


Figure (3.6) The arrangement of energy levels for  $^{228}\text{Th}$ , theoretical and experimental

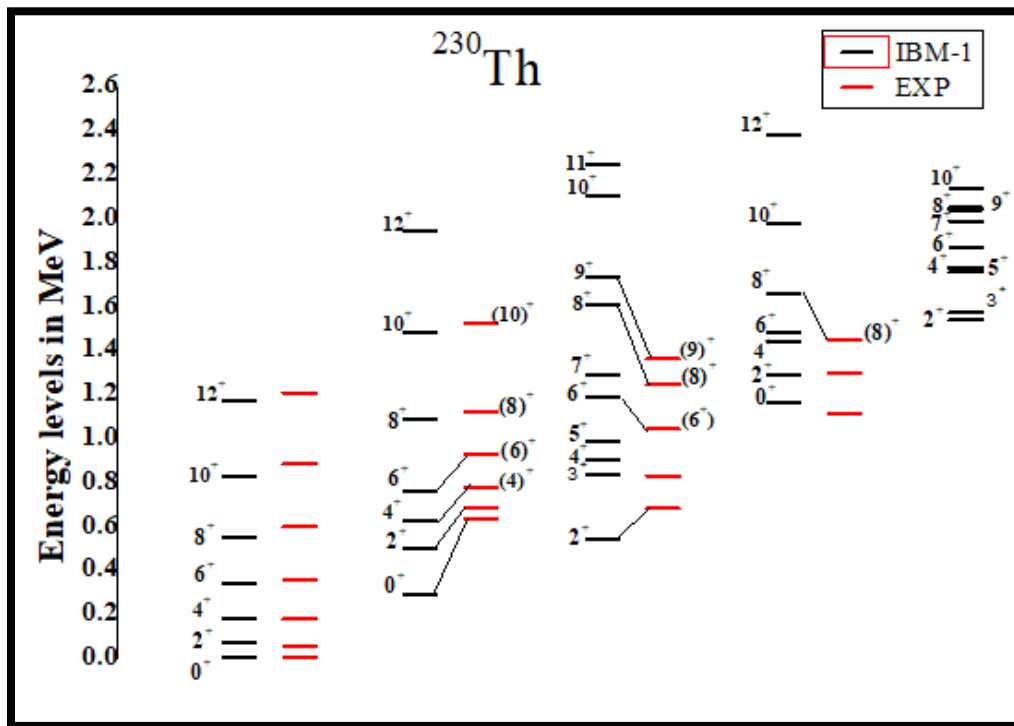


Figure (3.7) The arrangement of energy levels for  $^{230}\text{Th}$ , theoretical and experimental

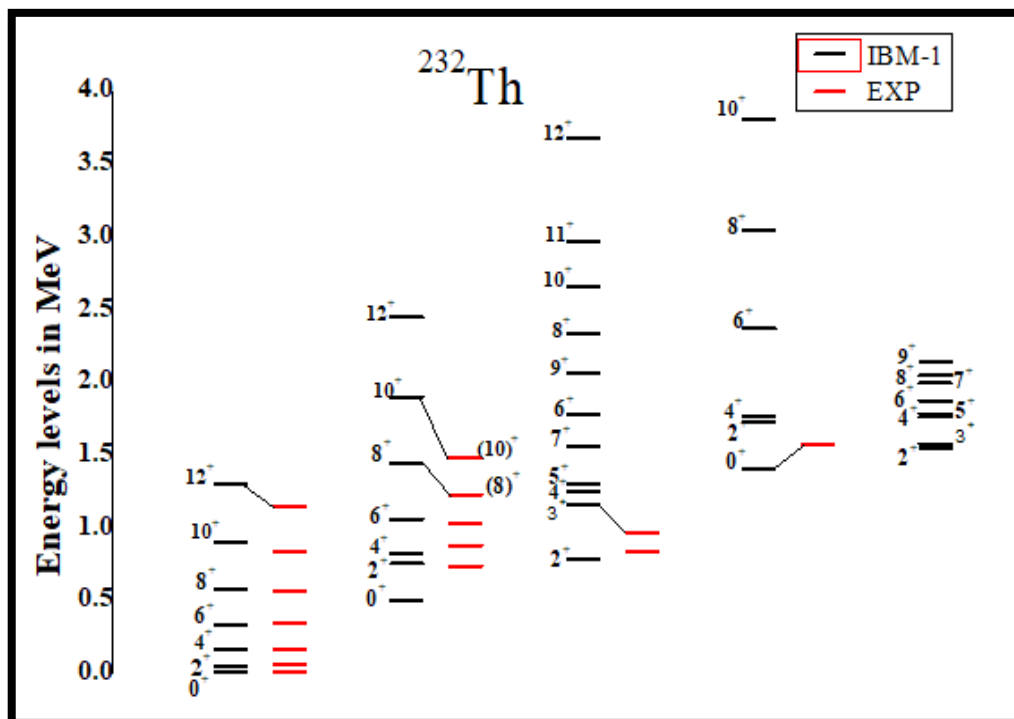
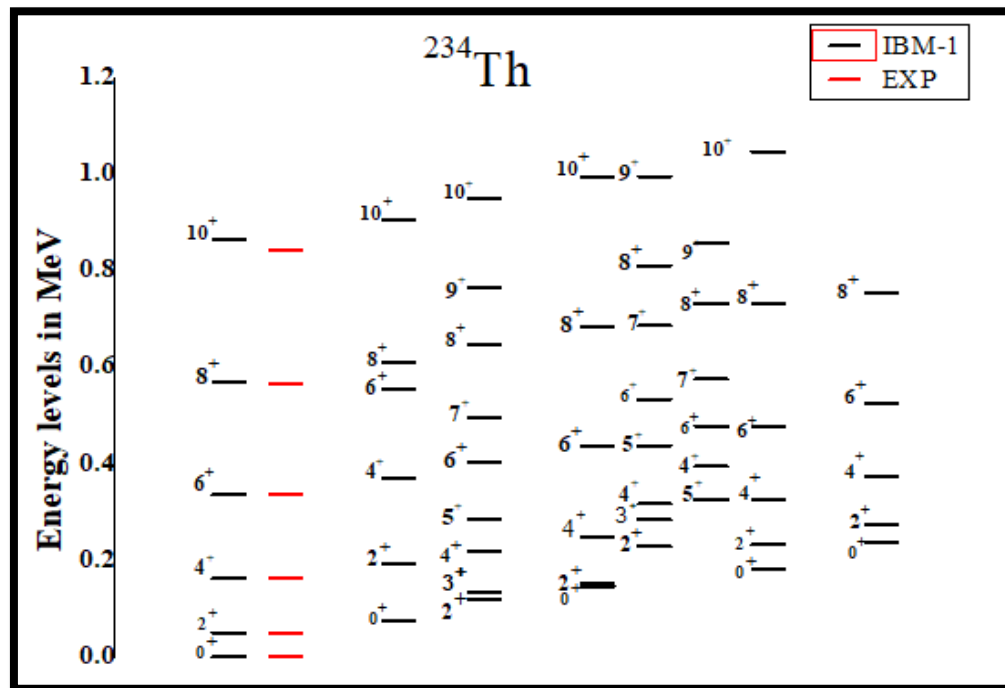


Figure (3.8) The arrangement of energy levels for  $^{232}\text{Th}$ , theoretical and experimental



**Figure (3.9)** The arrangement of energy levels for  $^{234}\text{Th}$ , theoretical and experimental

Figures (3.4),(3.5) and (3.9) have only ground band energy level ( $2_1, 4_1, 6_1, 8_1, \dots$ ), so the other bands were getting theoretical only. Figures (3.6), (3.7) and (3.8), have ground band also other bands, which there are a good divergence between the experimental and theoretical energy level.

### 3.3 B(E2) reduced electric transition:

In order to obtain a large amount of information about the nuclei, it was necessary to study the quadrupole electrical transitions using the (IBMT-1) program. Values were determined ( $\beta_2, \alpha_2$ ) in equation (2.4) and calculated from each isotope, then interred in the program with parameters in equations (3.1) and (3.2). In the current study, the parameters were determined based on the experimental values of the transitions mainly  $2_1^+ \rightarrow 0_1^+$ , where the coefficients were used E2SD and E2DD [89] which are:

$$E2SD = \alpha_2 \quad (3.1)$$

$$E2DD = \sqrt{5} \beta_2 \quad (3.2)$$

The values of  $B(E2)_{\downarrow}$  were calculated using the beneficial relation [90]:

$$B(E2)_{\downarrow} = \frac{(2I_f+1)}{(2I_i+1)} B(E2)_{\uparrow} \quad (3.3)$$

where  $I_i$  and  $I_f$  are the initial and final angular momentums .

Table (3.3) contain the first electric transition for all isotopes from data sheet and comparing with theoretical results [91] .

**Table (3.3):** B(E2) experimental data and its coefficients (E2SD, E2DD)

The isotopes	$B(E2; 2_1^+ \rightarrow 0_1^+)$ $e^2b^2$ [92]	B(E2) IBM -1	E2SD(eb)	E2DD(eb)
<sup>224</sup> Th	0.77614	0.76439	0.14329	-0.42386
<sup>226</sup> Th	1.341716	1.70954	0.18840	-0.55729
<sup>228</sup> Th	1.382405	1.430179	0.21324	-0.63079
<sup>230</sup> Th	1.641467	1.34394	0.26261	-0.77684
<sup>232</sup> Th	1.677470	1.27351	0.30527	-0.90301
<sup>234</sup> Th	1.568235	1.25995	0.34732	-1.02739

A comparison was made between our theoretical calculations and the experimental data for B(E2) obtained from reference [92]. are presented in tables (3.4-3.9) for <sup>224</sup>Th to <sup>234</sup>Th respectively.

**Table (3.4) :** Some electric transitions B(E2) for  $^{224}\text{Th}$ 

$J_i^+ \rightarrow J_f^+$	B(E2) $\downarrow e^2b^2$	
	Exp.	IBM-1
$2_1^+ \rightarrow 0_1^+$	0.77614	0.7643948
$2_1^+ \rightarrow 0_2^+$	--	0.0703174
$2_2^+ \rightarrow 0_1^+$	--	0.0828045
$2_2^+ \rightarrow 0_2^+$	--	0.0270447
$2_4^+ \rightarrow 0_1^+$	--	0.0044954
$2_4^+ \rightarrow 0_2^+$	--	0.0947594
$3_1^+ \rightarrow 2_1^+$	--	0.0855228
$3_1^+ \rightarrow 2_2^+$	--	0.7218213
$3_2^+ \rightarrow 2_1^+$	--	0.0016745
$4_1^+ \rightarrow 2_1^+$	--	1.0741140
$4_1^+ \rightarrow 2_2^+$	--	0.0249889
$4_2^+ \rightarrow 2_1^+$	--	0.1024267
$6_1^+ \rightarrow 4_1^+$	--	1.0869880
$6_2^+ \rightarrow 4_1^+$	--	0.0932690
$6_2^+ \rightarrow 4_2^+$	--	0.3090540
$Q (2_1^+ \rightarrow 2_1^+)$	--	-2.5429940

Table (3.4), contain some electric transition for allowed transition, and have great value  $4_1 \rightarrow 2_1, 6_1 \rightarrow 2_1$  transition and the some in table (3.5), become they belong the some limit . the quadrupole momentum Q has maximum value.

**Table (3.5) :** Some electric transitions B(E2) for  $^{226}\text{Th}$ 

$j_i^+ \rightarrow j_f^+$	B(E2) $\downarrow e^2b^2$	
	Exp.	IBM-1
$2_1^+ \rightarrow 0_1^+$	1.341716	1.7095460
$2_1^+ \rightarrow 0_2^+$	--	0.1313972
$2_2^+ \rightarrow 0_1^+$	--	0.1411555
$2_2^+ \rightarrow 0_2^+$	--	0.0394144
$2_4^+ \rightarrow 0_1^+$	--	0.0068477
$2_4^+ \rightarrow 0_2^+$	--	0.1959411
$3_1^+ \rightarrow 2_1^+$	--	0.1522735
$3_1^+ \rightarrow 2_2^+$	--	1.6783920
$3_2^+ \rightarrow 2_1^+$	--	0.0024018
$4_1^+ \rightarrow 2_1^+$	--	2.4107670
$4_1^+ \rightarrow 2_2^+$	--	0.0330782
$4_2^+ \rightarrow 2_1^+$	--	0.1893978
$6_1^+ \rightarrow 4_1^+$	--	2.4773540
$6_2^+ \rightarrow 4_1^+$	--	0.1853181
$6_2^+ \rightarrow 4_2^+$	--	0.7338289
$Q (2_1^+ \rightarrow 2_1^+)$	--	-3.7472110

**Table (3.6) :** Some electric transitions B(E2) for  $^{228}\text{Th}$ 

$j_i^+ \rightarrow j_f^+$	B(E2) $\downarrow e^2b^2$	
	Exp.	IBM-1
$2_1^+ \rightarrow 0_1^+$	1.382405	1.4301790
$2_1^+ \rightarrow 0_2^+$	--	0.1756768
$2_2^+ \rightarrow 0_1^+$	--	0.0123060
$2_2^+ \rightarrow 0_2^+$	--	0.3105225
$2_4^+ \rightarrow 0_1^+$	--	0.0107022
$2_4^+ \rightarrow 0_2^+$	--	0.0158947
$3_1^+ \rightarrow 2_1^+$	--	0.0001651
$3_1^+ \rightarrow 2_2^+$	--	0.2187000
$3_2^+ \rightarrow 2_1^+$	--	0.0000194
$4_1^+ \rightarrow 2_1^+$	2.003245	2.1667240
$4_1^+ \rightarrow 2_2^+$	--	0.0416354
$4_2^+ \rightarrow 2_1^+$	--	0.0364341
$6_1^+ \rightarrow 4_1^+$	--	2.4432050
$6_2^+ \rightarrow 4_1^+$	--	0.0336004
$6_2^+ \rightarrow 4_2^+$	--	0.0526180
$Q (2_1^+ \rightarrow 2_1^+)$	--	-3.4123760

**Table (3.7):** Some electric transitions B(E2) for  $^{230}\text{Th}$ 

$j_i^+ \rightarrow j_f^+$	B(E2) $\downarrow e^2b^2$	
	Exp.	IBM-1
$2_1^+ \rightarrow 0_1^+$	1.641467	1.3439470
$2_1^+ \rightarrow 0_2^+$	--	0.0502260
$2_2^+ \rightarrow 0_1^+$	0.02200	0.0828045
$2_2^+ \rightarrow 0_2^+$	--	0.0270447
$2_4^+ \rightarrow 0_1^+$	--	0.0044954
$2_4^+ \rightarrow 0_2^+$	--	0.0947594
$3_1^+ \rightarrow 2_1^+$	--	0.0855228
$3_1^+ \rightarrow 2_2^+$	--	0.7218213
$3_2^+ \rightarrow 2_1^+$	--	0.0016745
$4_1^+ \rightarrow 2_1^+$	1.613000	1.0741140
$4_1^+ \rightarrow 2_2^+$	--	0.0249889
$4_2^+ \rightarrow 2_1^+$	--	0.1024267
$6_1^+ \rightarrow 4_1^+$	--	1.0869880
$6_2^+ \rightarrow 4_1^+$	--	0.0932690
$6_2^+ \rightarrow 4_2^+$	--	0.3090540
$Q(2_1^+ \rightarrow 2_1^+)$	--	-2.5429940

**Table (3.8):** Some electric transitions B(E2) for  $^{232}\text{Th}$ 

$j_i^+ \rightarrow j_f^+$	B(E2) $\downarrow e^2b^2$	
	Exp.	IBM-1
$2_1^+ \rightarrow 0_1^+$	1.677470	1.2735120
$2_1^+ \rightarrow 0_2^+$	0.023000	0.0085507
$2_2^+ \rightarrow 0_1^+$	--	1.0959490
$2_2^+ \rightarrow 0_2^+$	--	0.5203701
$2_4^+ \rightarrow 0_1^+$	--	0.0002480
$2_4^+ \rightarrow 0_2^+$	--	0.4201611
$3_1^+ \rightarrow 2_1^+$	--	1.5094510
$3_1^+ \rightarrow 2_2^+$	--	1.8341710
$3_2^+ \rightarrow 2_1^+$	--	0.0122705
$4_1^+ \rightarrow 2_1^+$	2.01013	1.8070730
$4_1^+ \rightarrow 2_2^+$	--	0.3012578
$4_2^+ \rightarrow 2_1^+$	--	0.2607113
$6_1^+ \rightarrow 4_1^+$	2.91012	2.1536480
$6_2^+ \rightarrow 4_1^+$	--	0.6587607
$6_2^+ \rightarrow 4_2^+$	--	0.1285906
$Q (2_1^+ \rightarrow 2_1^+)$	--	-1.3896580

Table (3.6) and (3.7), contain some electric transition for allowed transition, and have great value  $4_1 \rightarrow 2_1, 6_1 \rightarrow 2_1$  transition and the some in table (3.8),

become they belong the some limit . the quadrupole momentum Q has maximum value.

**Table (3.9):** Some electric transitions B(E2) for  $^{234}\text{Th}$

$j_i^+ \rightarrow j_f^+$	B(E2) $\downarrow e^2b^2$	
	Exp.	IBM-1
$2_1^+ \rightarrow 0_1^+$	1.568235	1.2599520
$2_1^+ \rightarrow 0_2^+$	--	0.3491617
$2_2^+ \rightarrow 0_1^+$	--	4.6893370
$2_2^+ \rightarrow 0_2^+$	--	3.8342980
$2_4^+ \rightarrow 0_1^+$	--	0.0346503
$2_4^+ \rightarrow 0_2^+$	--	2.4097870
$3_1^+ \rightarrow 2_1^+$	--	6.3708930
$3_1^+ \rightarrow 2_2^+$	--	1.9009290
$3_2^+ \rightarrow 2_1^+$	--	0.0141268
$4_1^+ \rightarrow 2_1^+$	--	1.8781310
$4_1^+ \rightarrow 2_2^+$	--	0.7757772
$4_2^+ \rightarrow 2_1^+$	--	2.2223610
$6_1^+ \rightarrow 4_1^+$	--	2.5501720
$6_2^+ \rightarrow 4_1^+$	--	1.6613860
$6_2^+ \rightarrow 4_2^+$	--	6.8301500
$Q (2_1^+ \rightarrow 2_1^+)$	--	-0.0111643

Table (3.9) have more high value of transition because these transition are allowed.

We obtained a convergence between the theoretical and experimental probability of the first transition  $2_1^+$ , This source is proof of the validity of our work.

Figure (3.10) shows a good match between experimental and computed,  $B(E2; 2_1^+ \rightarrow 0_1^+)$  for all isotopes .

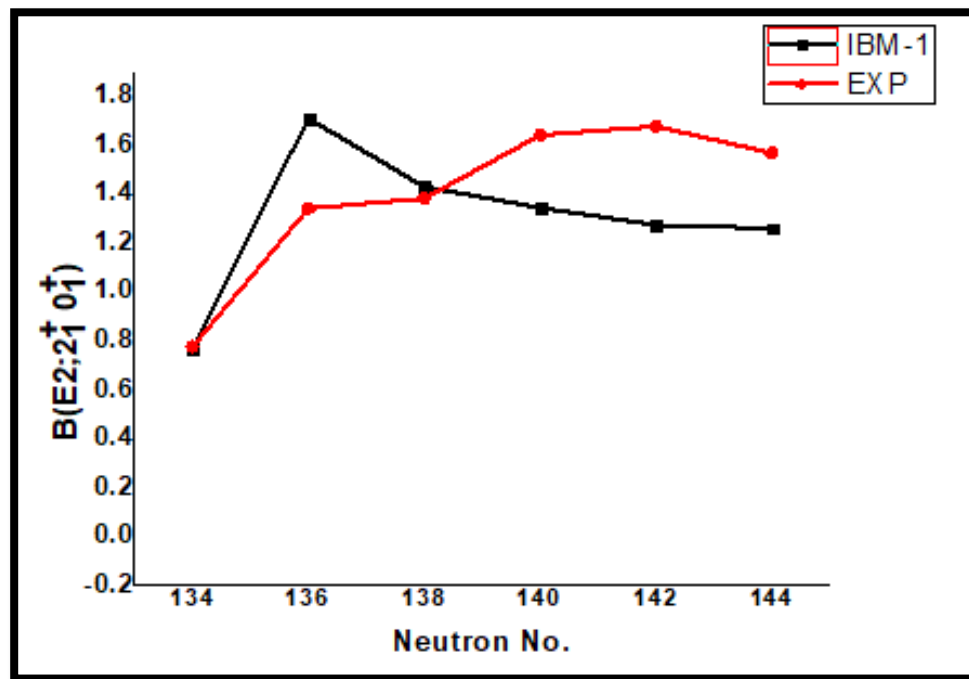


Figure (3.10)  $B(E2; 2_1^+ \rightarrow 0_1^+)$  comparison for all isotopes.

### 3.5 B(E2) Branching Ratios

Studying the branching ratios is important for understanding the dynamical symmetries and nucleus shape to which they belong, and defined as the ratio between two quadrupole electric as in table (3.10).

**Table (3.10):** Two electric transition branching ratios.

<i>The isotopes</i>	<i>R</i>		<i>R'</i>		<i>R''</i>	
	<i>EXP</i>	<i>IBM – 1</i>	<i>EXP</i>	<i>IBM – 1</i>	<i>EXP</i>	<i>IBM – 1</i>
<sup>224</sup> Th	---	1.40518	---	0.05741	---	0
<sup>226</sup> Th	---	1.41017	---	0.03021	---	0
<sup>228</sup> Th	1.44910	1.51500	---	0.09080	---	0
<sup>230</sup> Th	0.32372	1.12954	---	1.72646	---	0
<sup>232</sup> Th	0.40555	1.07726	6.70322	1.76586	---	0
<sup>234</sup> Th	---	1.19760	---	4.82819	---	0

Calculating the ratio  $R, R', R''$  for <sup>224</sup>Th, <sup>226</sup>Th and <sup>234</sup>Th which belongs to the transition region SU(3) and O(6) near to SU(3) applying equations (2.28),(2.29) and (2.30) respectively.

There are not experimental values for <sup>224</sup>Th, <sup>226</sup>Th and <sup>234</sup>Th because we don't have the transition  $B(E2: 4_1^+ \rightarrow 2_1^+)$ , but they exist for <sup>228</sup>Th, <sup>230</sup>Th and <sup>232</sup>Th .

### 3.6 Surface Potential Energy:

One of the characteristics of nuclei is the potential energy surface, which gives nuclei their distinct form. Potential energy surface  $E(N, \beta, \gamma)$  is calculated using the PES.FOR tool. In this study, equation (2.44,2.45) are used to compute the potential energy surface.

The IBMP-code's Hamiltonian parameters are displayed in table (3.11), these variables are taken from the potential energy surface equation, from the IBM program's output. All values in this table have  $A_4$  equal zero.

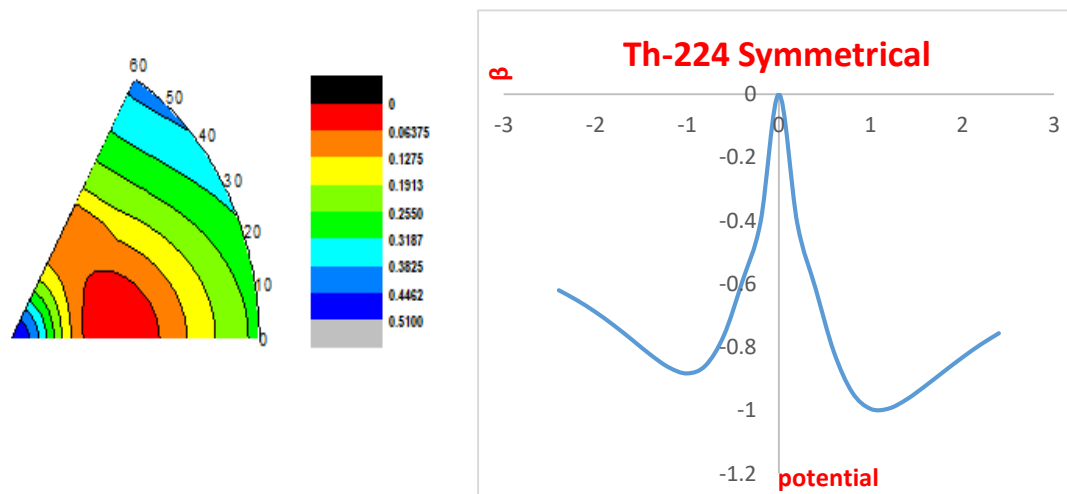
**Table (3.11):** The coefficients of potential energy as in IBM program.

The Isotopes	Boson Number	ES (MeV)	ED (MeV)	A1 (MeV)	A2 (MeV)	A3 (MeV)	A4 (MeV)
$^{224}\text{Th}$	8	-0.0510	0.0390	0.0000	-0.0040	-0.0410	0.0000
$^{226}\text{Th}$	9	-0.0340	0.0450	0.0000	-0.0030	-0.0280	0.0000
$^{228}\text{Th}$	10	-0.1210	0.2430	0.0570	-0.0250	-0.0970	0.0000
$^{230}\text{Th}$	11	-0.0910	0.1650	0.0510	0.0050	-0.0730	0.0000
$^{232}\text{Th}$	12	-0.1000	0.2480	0.0760	0.0210	-0.0800	0.0000
$^{234}\text{Th}$	13	-0.0130	0.0390	0.0010	0.0010	-0.0120	0.0000

The parameters in table (3.11) input in IBMP-code to get the potential energies various with the deformation from angle  $0^\circ$  to  $60^\circ$ , then the figure (3) represented the relation between potential energy surface and the deformation  $\beta$  in column a, and the surface contour of this relation in column b for all isotopes. From these plots it is clear there is some deformation in  $^{224}\text{Th}$ ,  $^{226}\text{Th}$ ,  $^{228}\text{Th}$ ,  $^{230}\text{Th}$ ,  $^{232}\text{Th}$  and  $^{234}\text{Th}$  because there are deviation in the values of the potential.

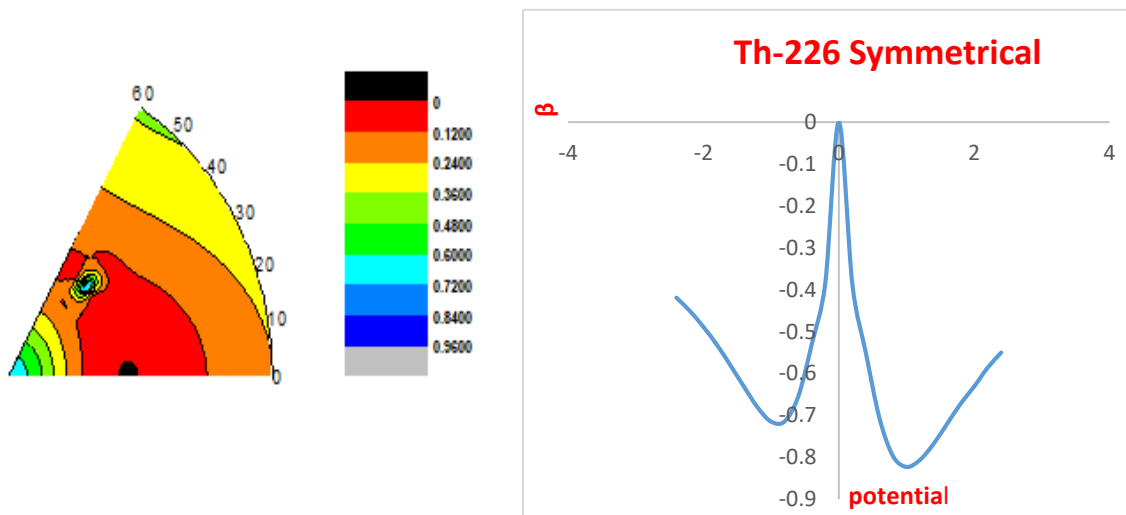
The values of deformation ( $\beta$ ) equal 0 to 2.4 and deviation angle ( $\gamma$ ) equal 0 to 60 according to solve equation(2.45).

Figures (3.11-3.16) represent the potential energy surface for ( $^{224}\text{Th}$ ,  $^{226}\text{Th}$ ,  $^{228}\text{Th}$ ,  $^{230}\text{Th}$ ,  $^{232}\text{Th}$  and  $^{234}\text{Th}$ ) respectively, as contour lines and symmetric shape of prolate ( $\gamma = 0$ ), and oblate ( $\gamma = 60$ ).



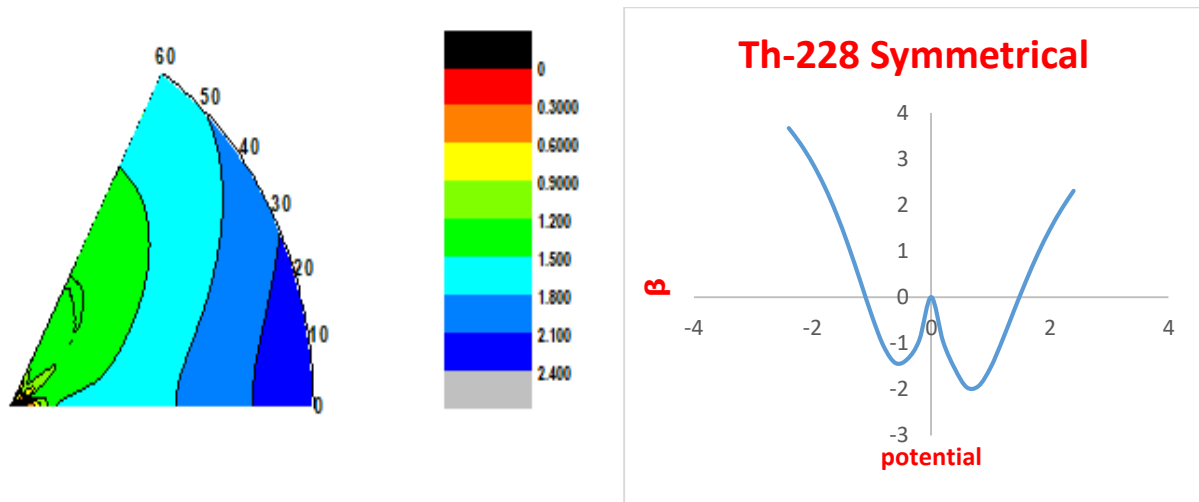
**Figure (3.11).** symmetric shape and potential distribution for  $^{224}\text{Th}$

The symmetric shape for two sides: prolate and oblate for  $^{224}\text{Th}$  and contour lines for the potential energy denoted in figure (3.11). There is asymmetry in both side because the deformation in the distribution of the potential in surface specially in  $30 < \gamma < 60$  and the maximum value of potential reach to 1 MeV, it showed that the maximum value of potential (0.375 MeV when  $\beta = 2.4$  and  $\gamma = 60^\circ$ ) and the minimum value of potential (0 MeV when  $\beta = 1.0$  and  $\gamma = 0^\circ$ ).



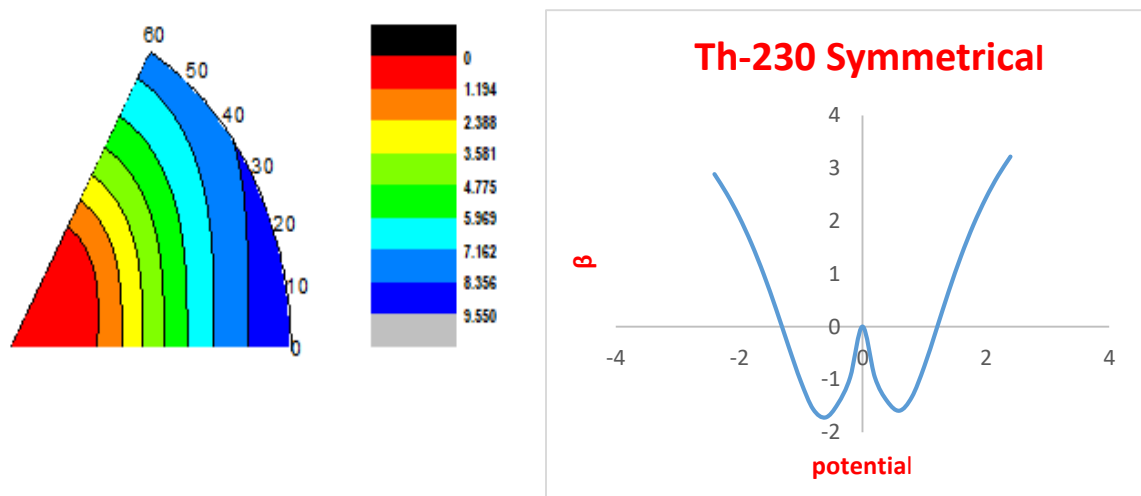
**Figure (3.12):** symmetric shape and potential distribution for  $^{226}\text{Th}$

Figure (3.12) represent to the potential for  $^{226}\text{Th}$ , which clear there is asymmetry in both sides and the potential gathered in  $\beta < 1$  and reach to 800 KeV , it showed that the maximum value of potential (0.509 MeV when  $\beta = 0$  and  $\gamma = 60^\circ$ ) and the minimum value of potential (0 MeV when  $\beta = 1.0$  and  $\gamma = 0^\circ$ )



**Figure (3.13):** symmetric shape and potential distribution for  $^{228}\text{Th}$

The last figure (3.13) for  $^{228}\text{Th}$ , refers to symmetry in both sides and equal distribution in contour lines approximately with high potential energy greater than 10 MeV, it showed that maximum value of potential (5.624 MeV when  $\beta=2.4$  and  $\gamma=60^\circ$ ) and the minimum value of potential (0 MeV when  $\beta=0.6$  and  $\gamma=0^\circ$ ).



**Figure(3.14).** symmetric shape and potential distribution for  $^{230}\text{Th}$

In figure (3.14) we notice a decrease in the potential energy on both the right and left sides by 1.9 Mev and by 2 Mev, it showed that the maximum value of potential (4.939 MeV when  $\beta= 2.4$  and  $\gamma= 0^\circ$  ) and the minimum value of potential (0 MeV when  $\beta= 0.6$  and  $\gamma= 60^\circ$ ).

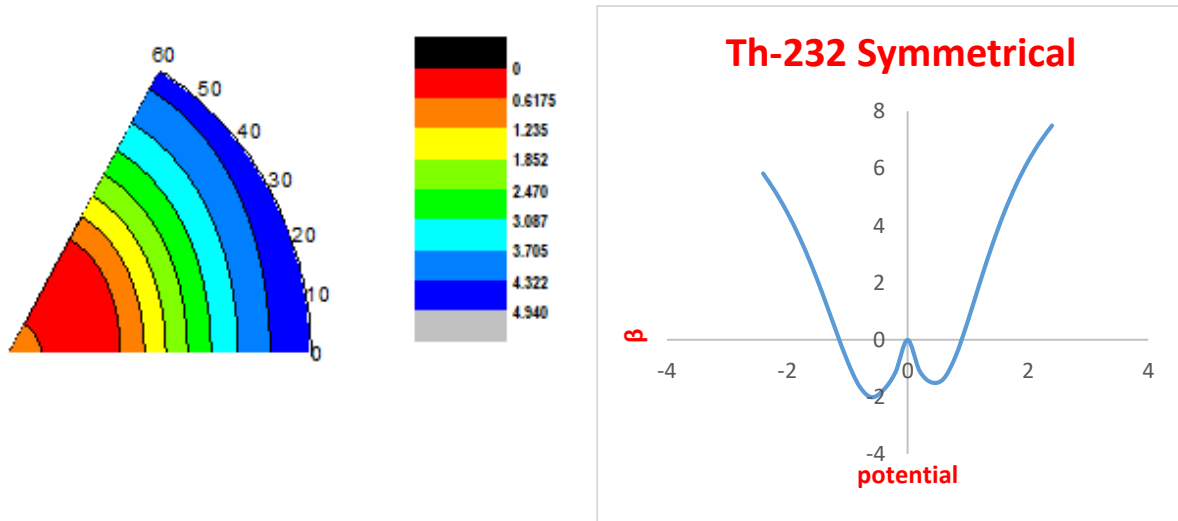


**Figure (3.15).** symmetric shape and potential distribution for  $^{232}\text{Th}$

In figure (3.15), so the figure is not symmetrical, as for the contour lines, compared to the standard lines, the lines are tortuous and distorted, and this distortion is the SU(3) distortion it showed that the maximum value of potential (9.510 MeV when  $\beta= 2.4$  and  $\gamma= 0^\circ$  ) and the maximum value of potential (0 MeV when  $\beta= 0.6$  and  $\gamma= 60^\circ$ ).

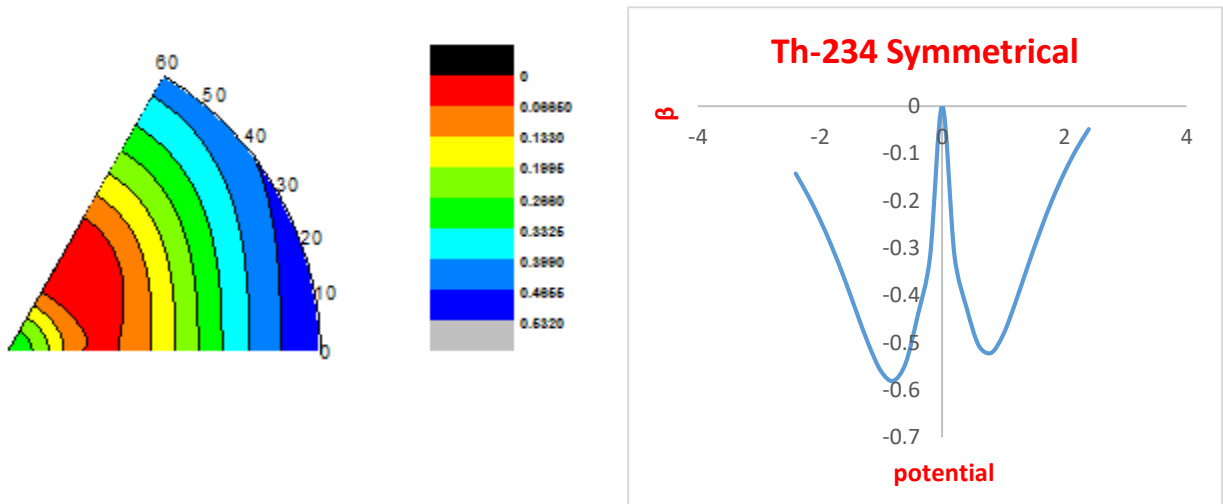


**Figure (3.16).** symmetric shape and potential distribution for  $^{234}\text{Th}$

In figure (3.16) There is asymmetry in both side because the deformation in the distribution of the potential in surface specially in  $30 < \gamma < 60$  and the maximum value of potential reach to 0.6 MeV. it showed that the maximum value of potential (0.532 MeV when  $\beta = 2.4$  and  $\gamma = 0^\circ$ ) and the that the minimum value of potential (0 MeV when  $\beta = 0.8$  and  $\gamma = 60^\circ$ ).

From the previous it becomes clear that this thorium series is a regular one with sequential properties, which are as follows:

- 1-  $^{224}\text{Th}$ : The first isotope contains several theoretical levels and matches the ground band found in the practical, and there are no other practical levels. This isotope contains a clear distortion through the potential contour drawings in comparison with the standard voltage diagram (2.5). We notice the gathering of the contour lines at  $0.4 < \beta < 1.2$  the potential in this place, which is called prolate rotor, from the energy ratios and the arrangement of the energy levels and potential energy surface, indicate that this isotope return to the transition region SU(3)-O(6).
- 2-  $^{226}\text{Th}$  : The second isotope contains several theoretical levels and matches the ground band found in the practical, and there are no other practical levels. This isotope contains a clear distortion through the potential contour drawings in comparison with the standard voltage diagram (2.5). We notice the gathering of the contour lines at  $0.4 < \beta < 1.2$  the potential in this place, which is called triaxial rotor, regarding the second isotope, it goes back to the transition region SU(3)-O(6), from the energy ratios, energy levels, branching ratios and potential energy surface.
- 3-  $^{228}\text{Th}$ : The third counterpart contains several theoretical levels that match the practical levels of the ground, first, and second bands, and also shows a clear distortion through the deviation of the contour lines from the standard lines. as for this isotope, Levels have been confirmed (102,31,51,91), it is considered pure SU(3), but the arrangement of beams

and energy can only be achieved by adding a term to the Hamiltonian, as shown previously.

- 4-  $^{230}\text{Th}$ : The fourth counterpart contains several theoretical levels that match the practical levels of the ground, first, and second bands, and also shows a clear distortion through the deviation of the contour lines from the standard lines. As for this isotope, levels have been confirmed (42,62,82,102,63,83,91,84), the energy, branching ratios and potential energy surface all explain the distortions present in this isotope, and this is evidence that the isotope belongs to SU(3). Also, the matching of energy levels only occurred by adding a term to the Hamiltonian.
- 5-  $^{232}\text{Th}$ : The fifth counterpart contains several theoretical levels that match the practical levels of the ground, first, and second bands, and also shows a clear distortion through the deviation of the contour lines from the standard lines. As for this isotope, levels have been confirmed (82,102,03), the properties for this isotope as the above one, the energy levels, branching ratios and potential energy surface all explain the distortions present in this isotope, and this is evidence that the isotope belongs to SU(3) with matching of energy levels only occurred by adding a term to the Hamiltonian.
- 6-  $^{234}\text{Th}$ : From the energy ratios and the arrangement of the energy levels and potential energy surface, they all indicate return this isotope to the transition region SU(3)-O(6).

## Chapter Four

### Discussion and Conclusions

The isotopes are part of the series of isotopes of the thorium element, which has (30) isotopes, and 6 isotopes were selected, which have excited and unknown energy levels.

#### Conclusions:

- A good agreement was obtained for the theoretical and practical energy levels using this model and for the low energy levels of these thorium isotopes.
- The congruence of some  $^{228}\text{Th}$ ,  $^{230}\text{Th}$  and  $^{232}\text{Th}$  isotopes was not obtained except by adding a limit that does not exist in the Hamiltonian, which is called symmetry breaking and gives us a correct arrangement, especially of the energy bands above the ground band.
- $^{224}\text{Th}$ ,  $^{226}\text{Th}$  and  $^{234}\text{Th}$  isotopes returns to the transition region between SU(3) and O(6).
- The three isotopes  $^{228}\text{Th}$ ,  $^{230}\text{Th}$  and  $^{232}\text{Th}$  counterparts belong to the determination SU(3) and contain many levels of uncertainties energy levels  $^{228}\text{Th}$  (10<sub>2</sub>,3<sub>1</sub>,5<sub>1</sub>,9<sub>1</sub>),  $^{230}\text{Th}$  (4<sub>2</sub>,6<sub>2</sub>,8<sub>2</sub>,10<sub>2</sub>,6<sub>3</sub>,8<sub>3</sub>,9<sub>1</sub>,8<sub>4</sub>),  $^{232}\text{Th}$  (8<sub>2</sub>,10<sub>2</sub>,0<sub>3</sub>) that were confirm in the theoretical results
- The electric quadrupole (Q) is a measure of the deviation of the nucleus from the spherical shape, all of our isotopes contain negative values, meaning they are all distorted.

- The branching ratios  $R, R', R''$  are another measure to know the shape of the nucleus, as it gives an idea of the limit to which the isotope is due in comparison with the standard values.
- By drawing the potential surface of the  $^{224}\text{Th}$ ,  $^{226}\text{Th}$  and  $^{234}\text{Th}$  isotopes, we conclude that these isotopes contain the obvious distortion in the symmetrical graphics in the negative part, asymmetry on both sides, and irregularity in the contour lines compared to the standard lines.
- As for the three isotopes,  $^{228}\text{Th}$ ,  $^{230}\text{Th}$  and  $^{232}\text{Th}$  contains a small part of the distortion, and this is evident in the symmetrical graphics in the positive and negative regions.
- There is relation shape between increase of the number of neutrons with the deformation.

## Future Works

We propose the following: other effort is needed to identify other features in this mass region.

1. Use IBM-2 instead of IBM-1 to calculate isotopes.
2. Use (IBFM-1) and (IBFM-2) models to study even-odd isotope nuclear structures

## References

---

1. W. Meyerhof, "Element of Nuclear Physics", McGraw Hill Book Company, New York, (1967).
2. A. Beser, Concepts of Modern Physics, McGraw Hill Book Company, New York, (1973).
3. B. Cohen, Concepts of Nuclear Physics, McGraw Hill Book Company, New York, (1971).
4. H. Enge, Introduction to Nuclear Physics, Addison Wesley, U.S.A, (1966).
5. F. Iachello, and A. Arima, "Boson symmetries in vibrational nuclei", Physics Letters B, Vol.53 ,No.4, pp.(309-312) ,(1974).
6. A. Arima and F. Iachello, "Interacting boson model of collective nuclear states IV ". The O(6) limit. Annals of Physics, Vol.123, No.2, pp.(468-492) ,(1979).
7. M. K. Al-Janaby, "A study of nuclear Structure of  $^{98-108}$  Ru even- even Isotopes by the IBM-1", (Doctoral dissertation, M. Sc. Thesis, Babylon University) (2005).
8. C. F. Von Weizsacker, Nucl. Annals of Physics, Vol. 6, No. 431, (1935).
9. R. Freedman and H. Young, "University Physics with Modern Physics", 11th international edition, Sears and Zemansky, 1633-4. ISBN0-8053-8768-4.
10. M. W. Kirson,. Mutual influence of terms in a semi-empirical mass formula. Nuclear Annals of Physics, Vol.798, No. (1-2), p.p. (29-60) (2008).
11. W. J. Elsasser, Nuclear Annals of Physics, Vol. 4, No. 549, (1933).
12. H. A. Enge, " Introduction to Nuclear Physy ", Addison Wesley U.S.A, (1983).

## References

---

13. R. R. Roy, and B. P. Nigam, "Nuclear Physics Theory and Experiment", John Willey and Sons, (1967)
14. O. Haxel, J. H. D. Jensen, and H. E. Suess, On the " magic numbers" in nuclear structure. *Physical Review*, Vol.75, No.11, p.1766, (1949).
15. Otsuka, T. "Emerging concepts in nuclear structure based on the shell model". *Physics*, Vol. 4, No.1, pp.(258-285),(2022)
16. K. S. Krane, " Introductory Nuclear Physic ", John Wiley and Sons, (1988).
17. J. Wood , K. Hegde , W . Nazarewicz ,M . Huyse and P . Vanduppen , " Physics of Reports " , Vol.215 , p.101 , (1992).
18. K. Abrahams, K. Allaart, a A. E. Dieperink, *Nuclear structure* (Vol. 67). Springer Science and Business Media, (2013)
19. J. K. Jabber ," Decay schemes from the (n,  $\gamma$ ) reaction on  $^{151}\text{Eu}$  and  $^{181}\text{Ta}$ " (Doctoral dissertation, University of London, Royal Holloway and Bedford New College (United Kingdom)),(1989)
20. P. M. Walker, G. D. Dracoulis, A. Johnston, and J. R. Leigh, "High-spin states and two-quasiparticle structure in  $^{172}\text{Hf}$ ". *Nuclear Physics A*, Vol. 293, No.3, pp. (481-508), (1977).
21. A. Arima , T. Ohtsuka, F. Iachello , and I. Talmi, " Collective nuclear states as symmetric couplings of proton and neutron excitations", *Physics Letters B*, Vol. 66, No.3, pp. (205-208) ,(1977).
22. F. Iachello, *Nuclear Physic A*, Vol. 369, p.233 (1983).

23. Solov'ev, V. G. "Pair Correlations and Structure of Deformed Nuclei", Structure of Complex Nuclei/Struktura Slozhnykh Yader/СТРУКТУРА СЛОЖНЫХ ЯДЕР: Lectures presented at an International Summer School for Physicists, Organized by the Joint Institute for Nuclear Research and Tiflis State University in Telavi, Georgian SSR, pp. (23-51),(1969)
24. L. S. Kisslinger and R. A. Sorensen, "Spherical Nuclei with Simple Residual Forces ", Review Model Physics, Vol.35, No.4, p.(853),(1963).
25. A. I. Levon , G. Graw , R. Hertenberg, S. Pascu , P. G. Thirolf, H. F. Wirth, , and P.Alexa, "0+ states and collective bands in  $^{228}\text{Th}$  studied by the (p, t) reaction", Physical Review C, Vol. 88, No.1, p. 014310, (2013)
26. A. Leviatan and D. Shapira, " Algebraic benchmark for prolate-oblate coexistence in nuclei", Racah Institute of Physics, The Hebrew University,(2016).
27. S. Sharma, "Study of Nuclear Structure of  $^{146}\text{Sm}$  Using Interacting Boson Model-1".
28. S. Y. Lee, Y. J. Lee, and J. H. Lee," The study of structure in  $^{224-234}\text{Th}$  nuclei within the framework IBM", In EPJ Web of Conferences, Vol. 146, p. 10016, EDP Sciences, (2017).
29. N. Al-Dahan, "Descriptive study of the even-even actinide nuclei  $^{230-234}\text{Th}$  isotopes using IBM-1". Chinese Physics C, Vol.41, No.6, p. 064105,(2017)
30. S. B. Doma, and H. S. El-Gendy, "A nuclear phenomenological study of the even-even Thorium Isotopes  $^{228-232}\text{Th}$  ", International Journal of Modern Physics E, Vol. 27, No.05, p.1850040,(2018).

- 31.** I. M. Ahmed, M. A. Al-Jubbori, H. H. Kassim, H. Y. Abdullah, and F. I. Sharrad, “Investigation of even–even  $^{220-230}\text{Th}$  isotopes within the IBM”, IVBM and BM. Nuclear Physics A, Vol. 977, pp. (34-48), (2018).
- 32.** K. Nomura, Rodríguez-Guzmán, R., Humadi, Y. M., Robledo, L. M., and García-Ramos, J. E. , “Octupole correlations in light actinides from the interacting boson model based on the Gogny energy density functional”, Physical Review C, Vo.102, No.6, p. 064326, (2020)
- 33.** Y. Q., Wu, W., Teng, X. J., Hou, Na, G. X., Y. Zhang, He, B. C., and Y. A. Luo, “Spectral fluctuations in the interacting boson model”, Chinese Physics C, Vol.46, No.10 , p.104101,(2022).
- 34.** D. D. Warner, Nuclear Physic A , Vol.522, No.1, (1991).
- 35.** C. De Coster, K., Heyde, B., Decroix, P., Van Isacker, J., Jolie, H., Lehmann, and J. L. Wood, “ Particle-hole excitations in the interacting boson model (I)” General structure and symmetries. Nuclear Physics A, Vol. 600, No.2, pp. (251-271), (1996)
- 36.** R. F., Casten, and D. D. Warner, “The interacting boson approximation”, Reviews of Modern Physics, Vol.60, No.2, p.389, (1988).
- 37.** I. Hossain, I. M., Ahmed, F. I., Sharrad, H. Y., Abdullah, A. D., Salman, and N. Al-Dahan, “Yrast states and B (E2) values of even  $^{100-102}\text{Ru}$  isotopes using interacting boson model (IBM-1)”, Chiang Mai J Sci, Vol.42, pp.(996-1004),(2015).
- 38.** H. R. Yazar, and I. Uluer, “Negative parity states and some electromagnetic transition properties of even-odd erbium isotopes”, Physical Review C, Vol.75, No.3, p. 034309, (2007).

39. A., Arima, and F. Iachello, "The interacting boson model", Annual Review of Nuclear and Particle Science, Vol. 31, No.1, pp. (75-105), (1981).
40. R. F. Casten, and D.D Warner, "The Interacting Boson Approximation", Reviews of Modern Physics, Vol.60, No.2, pp. (389-406),(1988).
41. J. L. Basdevant, J., Rich, and M., Spiro, Fundamentals in nuclear physics: From nuclear structure to cosmology. Springer Science and Business Media, (2005).
42. J. Proskurins, "The Study of Nuclear Shape Phase Transitions and Quantum Chaos in The Frameworks of Geometrical and Algebraic Models of Even-Even Nuclei", Ph.D, Thesis, University of Latvia,(2010).
43. I. M., Ahmed, and M. I. Muhammed, "The Evolution of  $^{146}\text{Nd}$ – $^{156}\text{Nd}$  Isotope States under the Framework of BM, IBM-1, IVBM and DG", ZANCO Journal of Pure and Applied Sciences, Vol.28, No.6, pp. (21-31), (2016).
44. A., Sethi, N. M., Hintz, D. N., Mihailidis, A. M., Mack, M., Gazzaly, K. W., Jones, and D. Goutte, "Inelastic proton scattering from Pt isotopes and the interacting boson model", Physical Review C, Vol.44, No.2, p.700,(1991).
45. W. T., Chou, D. S., Brenner, R. F., Casten, and R. L. Gill, "Level lifetime measurements and the structure of neutron-rich Ge 78", Physical Review C, Vol.47,No.1, p.157,(1993).
46. J.Engel, and F. Iachello, "Interacting boson model of collective octupole states. Pt. 1", The rotational limit. Nuclear Physic A;(Netherlands), Vol.472, No.1, (1987).
47. Gh. A. Jaber and M. K. .Al-Jnaby, "Nuclear Structure for Some Even-Even (Kr, Xe, Hg) Nuclei Using IBM1,2",Ph.D.thesis, University of Babylon,(2022)

48. G. A. H. Jaber, and M. K. Muttaleb,” Studying the Isotopes nearby Closed Shell of Kr, Xe and Hg Using Interacting Boson Models”, Journal of University of Babylon for Pure and Applied Sciences, Vol.28, No.1, pp. (173-183),(2020)
49. N. A. Sallal, “Low-Lying Spectra and (E2) Transition Rate in Even-Even  $^{128-156}\text{Nd}$  Isotopes Using IBM-1”, M.Sc. thesis, University of Babylon,(2017).
50. G. A. Jaber, and M. K. Muttaleb,” Study the deformation in some even krypton isotopes (88-92) using IBM-1 model”, In Journal of Physics: Conference Series (Vol. 1234, No. 1, p. 012025). IOP Publishing,(2019).
51. A. Arima and F. Iachello, “The Interacting Boson Model”, Cambridge University Press, Cambridge, UK, (1987).
52. H. A . Marhoon , “ Study of the energy levels for even-even  $^{98-104}\text{Mo}$  by using IBM-1”, M.Sc. Thesis , Babylon University, (2010).
53. K. Nomura, “Interacting boson model with energy density functional” In Journal of Physics: Conference Series (Vol. 445, No. 1, p. 012015). IOP Publishing, (2013).
54. L., Frankfurt, and M. Strikman, “Hard nuclear processes and microscopic nuclear structure”, Physics Reports, Vol.160, No.5-6, pp. (235-427),(1988).
55. G. A. H., Jaber, and M. K. Muttale, “Effect The Change in Bosons on The Properties of Xenon Isotopes”,(2019). مؤتمرات الآداب والعلوم الانسانية والطبيعية.
56. P. Cejnar and J. Jolie, “Quantum phase transitions in the interacting boson model” , Progress in Particle and Nuclear Physics, Vol.62,No.1, pp.(210-256),(2009).

## References

---

57. K. S. Krane, “E2, M1 multipole mixing ratios in odd-mass nuclei,  $59 \leq A \leq 149$ ”, Atomic Data and Nuclear Data Tables, Vol.19, No.4, pp. (363-416),(1977).
58. O. Scholten, “The interacting boson approximation model and applications” Rijksuniversiteit Groningen (The Netherlands),(1980).
59. M. K. Mohammed, “A study of nuclear structure of  $^{130-150}\text{Ce}$  even-even isotopes by the interacting boson model-1” ,thesis, University of Babylon,(2015)
60. J. P. Elliott, “The interacting boson model of nuclear structure”, Reports on Progress in Physics, Vol.48, No.2, p.171,(1985).
61. O., Castanos, E., Chacón, A., Frank, and M. Moshinsky, “ Group theory of the interacting Boson model of the nucleus”. Journal of Mathematical Physics, Vol. 20, No.1, pp.(35-44),(1979).
62. A. Leviatan, “Partial dynamical symmetries” Progress in Particle and Nuclear Physics, Vol.66, No.1, pp.(93-143),(2011).
63. J., Engel, and F. Iachello, “Interacting boson model of collective octupole states:(I)”,The rotational limit. Nuclear Physics A, Vol. 472, No.1, pp.(61-84),(1987).
64. A. Arima and F. Iachello, “Interacting boson model of collective nuclear states II. the rotational limit”, Annals of Physics, Vol.111,No.1, pp.(201-238),(1978).
65. Kota, V. K. B., and Sahu, R. Structure of medium mass nuclei: deformed shell model and spin-isospin interacting boson model. CRC Press.(2016)
66. Warner, D. D., and Casten, R. F. Interacting-boson-approximation E 2 operator in deformed nuclei. Physical Review C, Vol. 25, No.4, p. (1982).

67. D. Bondatsos and E. David , “Interacting boson models of nuclear Structure”, Stanford , Pub. , In the United State, By Oxford University Press, New York,(1988).
68. D. D., Warner, and R. F. Casten, “Predictions of the interacting boson approximation in a consistent Q framework” *Physical Review C*, Vol.28, No.4, p.1798,(1983).
69. A. A. Mehdi, “Investigation of nuclear structure for isotopes  $^{114-132}\text{Te}$  even-even using interacting boson model-1”, M.Sc. Thesis, Babylon University,(2020).
70. A. Y. Kazem, “A study of nuclear properties of  $^{148-154}\text{Sm}$  even-even isotopes by the interacting boson model-1 (IBM-1)”, M.Sc. Thesis, Babylon University,(2010).
71. P., Cejnar, J., Jolie, and R. F. Casten, “Quantum phase transitions in 9the shapes of atomic nuclei”. *Reviews of Modern Physics*, Vol. 82 , No.3, p.2155.,(2010).
72. N. Turkan, Search for E (5) behavior,”IBM and Bohr–Mottelson model with Davidson potential calculations of some even–even Xe isotopes”, *Journal of Physics G: Nuclear and Particle Physics*, Vol.34,No.11, p.2235,(2007)
73. D. Warner, “A triple point in nuclei”, *Nature*, Vol. 420, No.6916, pp.(614-615),(2002).
74. A. Y. Shaalan, “Study of the electromagnetic transition and mixing ratio for some even-even nuclie”, M.Sc. Thesis, Babylon University,(2019).

## References

---

75. Y. D., Devi, and V. K. B. Kota, “sdg interacting boson model: hexadecupole degree of freedom in nuclear structure”, *Pramana*, Vol.39, pp. (413-491),(1992).
76. I. K. Jabir,”A study of nuclear properties of  $^{112-130}\text{Xe}$  even-even isotopes by the interacting boson model-1 (IBM-1)”, M.Sc. Thesis , Babylon University,(2016).
77. A. M., Khalaf, and T. M. d Awwad, “A theoretical description of U (5)-SU (3) nuclear shape transitions in the interacting boson model”, *Progress in Physics*, Vol.1, pp(7-11),(2013).
78. P., Christmas, and P. Cross, “Relative intensities of  $\gamma$ -rays from E2 transitions in the decay of  $^{180\text{m}}\text{Hf}$ ”, *Nuclear Instruments and Methods*, Vol.174, No.3, pp. (571-575),(1980).
79. F. Iachello, ,and A. Arima, “the Interacting Boson Model” (Cambridge University, Cambridge, England, 1987); F. Iachello and I. Talmi. *Review Model Physical*, Vol.59, No.339,(1987).
80. P., Van Isacker, and J. Q. Chen, “Classical limit of the interacting boson Hamiltonian”, *Physical Review C*, Vo.24, No.2, p. 684,(1981).
81. C. Leclercq and V. Shirly, *Tabele of Isotopes*, Wiley , New York,(1978).
82. A.E. Ignatovich, E.N. Shurshikov and Yu.F. Jaborov, *Nuclear Data Sheets* , Vol. 52, No. 2 , P. 365,(1987).
83. W. Chou, N. Zamfir, and R. Casten, *Physical Review C*,Vol.92 , No.1,(2000)
84. A. Bohr and B.R. Mottelson ,*Nuclear Structure*, Banjamine, Vol. 1.(1969)
85. Zhou Chunmei, *Nuclear Data Sheets*, Vol. 50, No. 2 , P. 351,(1987)
86. E. Browne, *Nuclear Data Sheets*, Vol. 52, No. 1, P. 127,(1987).

## References

---

87. A. K., Jain, B., Maheshwari, S., Garg, M., Patial, and B. Singh, “Atlas of nuclear isomers”. Nuclear Data Sheets, Vol.128, pp.(1-130),(2015).
88. I. M. Ahmed and M. I. M. Mustafa, “ The Evolution of  $^{146}\text{Nd}$ - $^{156}\text{Nd}$  Isotope States under the Framework of BM, IBM-1, IVBM and D-G”, ZANCO Journal of Pure and Applied Sciences, Vol. 28, No. 6, pp. (21-31),(2017).
89. P. J. Brussaard and P. W. M. Glaudemans, “Shell-Model Applications in Nuclear Spectroscopy”, North Holland Publishing Company, North Holland,(1977).
90. K.S. Krane and J. M. Shobaki , J., Physical Review C, Vol. 16, No. 4,(1977).
91. J.K. Tuli, Nuclear Data Sheets, Vol. 11, No.1, p. (12),(1998).
92. S. Raman, C. W. Nestor Jr, & P. Tikkanen, “ Transition probability from the ground to the first-excited  $2+$  state of even–even nuclides”, Atomic Data and Nuclear Data Tables, Vol.78, No.1, pp.(1-128),(2001).

## المخالصة

تم استخدام نموذج البوزونات المتفاعلة (IBM-1) للعثور على افضل هاملتوني لحساب قيم مستويات الطاقة والاحتمالية المختزلة للانتقال الكهربائي رباعي الأقطاب  $B(E2)$  وطاقة الجهد لأنوية نظائر زوجية- زوجية مختلفة مع الحصول على التطابق الجيد.

تم حساب مستويات الطاقة،  $B(E2)$ ، وعزم رباعي القطب الكهربائي للمستويات لعدد من الانتقالات للنظائر الزوجية- الزوجية ( $^{224}\text{Th}$ ,  $^{226}\text{Th}$ ,  $^{228}\text{Th}$ ,  $^{230}\text{Th}$ ,  $^{232}\text{Th}$ ,  $^{234}\text{Th}$ ) باستخدام أفضل المعاملات الملائمة في معادلة الهاملتوني باستخدام نموذج البوزونات المتفاعلة (IBM-1).  
1.)

وكذلك تحديد شكل النواة عن طريق دراسة طاقة جهد السطح باستخدام معادلات دالة الهاملتوني للجهد والذي يعطي فكرة عن التشوه الذي يحدث في النواة من انحراف الخطوط الكنتورية وتجميعها في منطقة معينة.

تم حساب نسب التفرع ( $R'$  و  $R'$  و  $R$ ) موقع العناصر بالنسبة للتحديدات الثلاثة  $SU(3)$  و  $O(6)$  و  $U(5)$  مهم في تحديد شكل النواة والتشوه الذي يحدث فيها. أظهرت النتائج أن النظائر ( $^{226}\text{Th}$ ,  $^{224}\text{Th}$ ) تقع في المنطقة الانتقالية  $SU(3) - O(6)$ ، تقع النظائر  $^{228}\text{Th}$ ,  $^{230}\text{Th}$ ,  $^{232}\text{Th}$  في التحديد  $SU(3)$ ، والنظير  $^{234}\text{Th}$  يقع في المنطقة الانتقالية  $SU(3) - O(6)$ .



جمهورية العراق  
وزارة التعليم العالي والبحث العلمي  
جامعة بابل / كلية العلوم  
قسم الفيزياء

## دراسة الخواص النووية لنظائر $^{224}\text{Th}$ - $^{234}\text{Th}$ الزوجية – الزوجية باستعمال (IBM-1)

رسالة مقدمة الى

مجلس كلية العلوم – جامعة بابل

و هي جزء من متطلبات نيل درجة الماجستير في علوم الفيزياء

من قبل

نبراس حيدر حمود عطية

بكالوريوس في علوم الفيزياء (٢٠١٨)

بأشراف

م.د.

غيداء عبد الحافظ جابر حسين

ا.د.

محسن كاظم مطلب الجنابي

م ٢٠٢٣

٥ ١٤٤٥

